

Shear-strain and shear-stress fluctuations in generalized Gaussian ensemble simulations of isotropic elastic networks

J.P. Wittmer,^{1,*} I. Kriuchevskiy,¹ J. Baschnagel,¹ and H. Xu²

¹*Institut Charles Sadron, Université de Strasbourg & CNRS,
23 rue du Loess, 67034 Strasbourg Cedex, France*

²*LCP-A2MC, Institut Jean Barriol, Université de Lorraine & CNRS, 1 bd Arago, 57078 Metz Cedex 03, France*
(Dated: June 14, 2021)

Shear-strain and shear-stress correlations in isotropic elastic bodies are investigated both theoretically and numerically at either imposed mean shear-stress τ ($\lambda = 0$) or shear-strain γ ($\lambda = 1$) and for more general values of a dimensionless parameter λ characterizing the generalized Gaussian ensemble. It allows to tune the strain fluctuations $\mu_{\gamma\gamma} \equiv \beta V \langle \delta\hat{\gamma}^2 \rangle = (1-\lambda)/G_{\text{eq}}$ with β being the inverse temperature, V the volume, $\hat{\gamma}$ the instantaneous strain and G_{eq} the equilibrium shear modulus. Focusing on spring networks in two dimensions we show, e.g., for the stress fluctuations $\mu_{\tau\tau} \equiv \beta V \langle \delta\hat{\tau}^2 \rangle$ ($\hat{\tau}$ being the instantaneous stress) that $\mu_{\tau\tau}|_{\lambda} = \mu_{\text{A}} - \lambda G_{\text{eq}}$ with $\mu_{\text{A}} = \mu_{\tau\tau}|_{\lambda=0}$ being the affine shear-elasticity. For the stress autocorrelation function $C_{\tau\tau}(t) \equiv \beta V \langle \delta\hat{\tau}(t)\delta\hat{\tau}(0) \rangle$ this result is then seen (assuming a sufficiently slow shear-stress barostat) to generalize to $C_{\tau\tau}(t)|_{\lambda} = G(t) - \lambda G_{\text{eq}}$ with $G(t) = C_{\tau\tau}(t)|_{\lambda=0}$ being the shear-stress relaxation modulus.

PACS numbers: 05.70.-a, 05.20.Gg, 05.10.Ln, 65.20.-w

I. INTRODUCTION

Background. A “simple average” $A = \langle \hat{A} \rangle$ of an observable \mathcal{A} [1] does not depend on which thermodynamic ensemble it is measured in, at least not if the system is sufficiently large and if each ensemble samples indeed the same thermodynamic state point [1–6]. An example for such a simple average is the affine shear-elasticity μ_{A} characterizing the energy change of an affinely shear-strained elastic body [7–10] as properly defined below in sect. III. As one may verify numerically [8], it is irrelevant whether one computes μ_{A} in the $NV\gamma T$ -ensemble at constant particle number N , volume V , shear strain γ and temperature $T \equiv 1/\beta$ or in the conjugated $NV\tau T$ -ensemble where the strain is allowed to fluctuate subjected to the constraint that the internal mean shear stress τ is imposed by the external applied shear stress τ_{ext} [3]. In contrast to this, the fluctuation $\langle \delta\hat{A}\delta\hat{B} \rangle$ of two observables \mathcal{A} and \mathcal{B} may depend on whether an extensive variable X or its conjugated intensive variable I is imposed [1–3]. Focusing in the present work on shear-strained isotropic elastic networks, as sketched in panel (a) of fig. 1, the relevant extensive variable is the rescaled shear strain $X = V\gamma$ and the conjugated intensive variable the shear stress $I = \tau$. Using the Lebowitz-Percus-Verlet (LPV) transform [2] it is seen for the (rescaled) mean-squared fluctuation $\mu_{\tau\tau} \equiv \beta V \langle \delta\hat{\tau}^2 \rangle$ of the instantaneous shear stress $\hat{\tau}$ that [8, 9]

$$\mu_{\tau\tau}|_{\lambda=0} = \mu_{\tau\tau}|_{\lambda=1} + G_{\text{eq}} \quad (1)$$

with G_{eq} being the equilibrium shear modulus. For later convenience the $NV\tau T$ -ensemble is indicated by “ $\lambda = 0$ ”

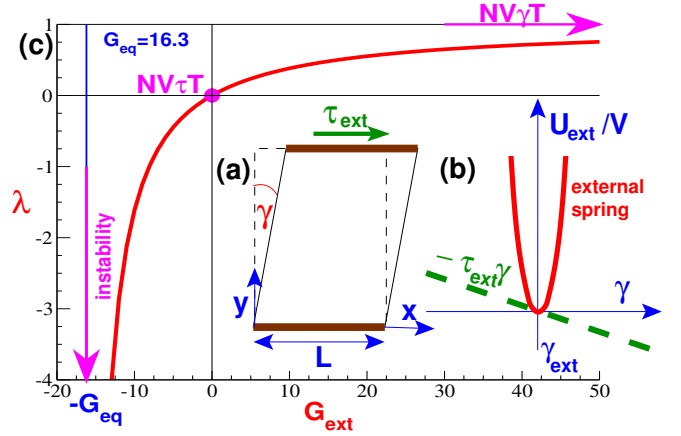


FIG. 1: Sketch of addressed problem: (a) Shear strain experiment in the (x, y) -plane with shear strain γ and applied external shear stress τ_{ext} . (b) External potential $U_{\text{ext}}(\gamma)/V$ according to eq. (3) with the bold line indicating the external spring of spring constant G_{ext} . (c) Dimensionless parameter $\lambda = G_{\text{ext}}/(G_{\text{eq}} + G_{\text{ext}})$ comparing the external spring constant G_{ext} and the equilibrium shear modulus G_{eq} . We set $G_{\text{eq}} = 16.3$ as for the elastic model system considered below.

and the $NV\gamma T$ -ensemble by “ $\lambda = 1$ ”. Generalizing eq. (1) in the time-domain it has been shown for the stress-stress correlation function $C_{\tau\tau}(t) \equiv \beta V \langle \delta\hat{\tau}(t)\delta\hat{\tau}(0) \rangle$ that [9, 10]

$$C_{\tau\tau}(t)|_{\lambda=0} = C_{\tau\tau}(t)|_{\lambda=1} + G_{\text{eq}}. \quad (2)$$

This assumes that the shear-barostat needed to sample the $NV\tau T$ -ensemble must act very slowly on the time-scales used to probe $C_{\tau\tau}(t)|_{\lambda=0}$. This may be realized equivalently by averaging over an ensemble of configurations with quenched strains $\hat{\gamma}$ distributed according to the $NV\tau T$ -ensemble [9]. It is due to the ergodicity breaking generated by the averaging over the quenched ensemble.

*Electronic address: joachim.wittmer@ics-cnrs.unistra.fr

ble that $C_{\tau\tau}(t)|_{\lambda=0} \rightarrow G_{\text{eq}}$ stays finite for $t \rightarrow \infty$, while $C_{\tau\tau}(t)|_{\lambda=1}$ must vanish for large times (as one commonly expects for all correlation functions in ergodic systems [11]). By integration by parts it is seen that $C_{\tau\tau}(t)|_{\lambda=0}$ is equivalent to the experimentally important shear relaxation modulus $G(t)$ [9]. The transform eq. (2) thus implies $G(t) = G_{\text{eq}} + C_{\tau\tau}(t)|_{\lambda=1}$, i.e. the relaxation modulus may be measured using the equilibrium modulus G_{eq} and the correlation function $C_{\tau\tau}(t)|_{\lambda=1}$ both determined in the NV γ T-ensemble [9].

Generalized Gaussian ensemble. As sketched in panel (b) of fig. 1, it is straightforward to interpolate between the NV γ T-ensemble and the NV τ T-ensemble by imposing an external field

$$U_{\text{ext}}(\hat{\gamma})/V = -\tau_{\text{ext}}(\hat{\gamma} - \gamma_{\text{ext}}) + \frac{1}{2}G_{\text{ext}}(\hat{\gamma} - \gamma_{\text{ext}})^2 \quad (3)$$

with G_{ext} being the spring constant of the external harmonic spring. The standard NV τ T-ensemble at $\tau = \tau_{\text{ext}}$ is recovered by setting $G_{\text{ext}} = 0$. Note that our approach is conceptually similar to the so-called ‘‘Gaussian ensemble’’ proposed some years ago by Hetherington and others [12, 13] generalizing the Boltzmann weight of the canonical ensemble by an exponential factor $U_{\text{ext}}(\hat{E}) \propto \hat{E}^2$ of the instantaneous energy \hat{E} . A similar external spring potential has been also used in the recent ‘‘elastic bath’’ approach by Workum and de Pablo [14]. Choosing the reference strain γ_{ext} equal to the mean strain γ_0 of the NV τ T-system at vanishing shear stress $\tau = \langle \hat{\tau} \rangle = \tau_{\text{ext}} \equiv 0$ allows to work at constant zero mean shear stress irrespective of the strength of the external potential [15]. All the ensembles considered correspond thus to the *same* thermodynamic state, i.e. all first derivatives of the energy or the free energy [3] and all simple averages are identical. As sketched in panel (c) of fig. 1, G_{ext} is not necessarily positive, reducing the strain fluctuations, but may even become negative, which thus amplifies the fluctuations. It has been argued [14] that this may allow a more convenient determination of the elastic modulus. Since the external spring is parallel to the system, the combined system and external device have an effective spring constant $G_{\text{eff}} = G_{\text{eq}} + G_{\text{ext}}$. Defining the dimensionless parameter $\lambda \equiv G_{\text{ext}}/(G_{\text{eq}} + G_{\text{ext}})$ the strain fluctuations of the combined system are thus given by

$$\mu_{\gamma\gamma} \equiv \beta V \langle \delta\hat{\gamma}^2 \rangle = 1/G_{\text{eff}} = (1 - \lambda)/G_{\text{eq}}, \quad (4)$$

i.e. must vanish linearly with λ . NV τ T-ensemble statistics is expected for $\lambda \rightarrow 0$, while NV γ T-statistics should become relevant in the opposite limit for $G_{\text{ext}} \rightarrow \infty$, i.e. $\lambda \rightarrow 1$. The system must become unstable in the limit $G_{\text{ext}} \rightarrow -G_{\text{eq}}$, i.e. $\lambda \rightarrow -\infty$.

Key results. The aim of the present study is to generalize the relations for static fluctuations, eq. (1), and dynamical correlation functions, eq. (2), to the more general transformations between Gaussian ensembles characterized by the continuous parameter $\lambda \leq 1$. In this way we want to make manifest that these transformation

relations are generated by the *continuous change* of the constraint imposed on the fluctuations of the extensive variable. Focusing on spring networks in two dimensions we show, e.g., for the stress-stress fluctuations $\mu_{\tau\tau}$ in different λ ensembles that

$$\mu_{\tau\tau}|_{\lambda} = \mu_{\tau\tau}|_{\lambda=0} - \lambda G_{\text{eq}} \quad (5)$$

with $\mu_{\tau\tau}|_{\lambda=0}$ being given by the affine shear-elasticity μ_{A} mentioned above. Assuming a very slowly acting shear-barostat, which is irrelevant for the system evolution for short times $t \ll \tau_*(\lambda)$, the above result is then seen to generalize in the time-domain for the stress-stress correlation function

$$C_{\tau\tau}(t)|_{\lambda} = C_{\tau\tau}(t)|_{\lambda=0} - \lambda G_{\text{eq}} \text{ for } t \ll \tau_*(\lambda). \quad (6)$$

Since $G(t) = C_{\tau\tau}(t)|_{\lambda=0}$, eq. (6) allows the determination of the relaxation modulus $G(t)$ from the equilibrium modulus G_{eq} and the stress-stress correlation function $C_{\tau\tau}(t)|_{\lambda}$ for any λ and $t \ll \tau_*(\lambda)$. The upper time limit $\tau_*(\lambda)$ is seen to be set by the diffusion time $T_{\gamma\gamma}$ of the instantaneous strain $\hat{\gamma}(t)$ over the typical strain fluctuations for λ . As a consequence from eq. (5) and eq. (6) it appears that it is the equilibrium modulus G_{eq} of the system, which generates both transforms

$$\frac{d}{d\lambda} \mu_{\tau\tau}|_{\lambda} = \frac{d}{d\lambda} C_{\tau\tau}(t)|_{\lambda} = -G_{\text{eq}} \quad (7)$$

with $\mu_{\tau\tau}|_{\lambda} = \mu_{\text{A}}$ and $C_{\tau\tau}(t)|_{\lambda} = G(t)$ for $\lambda = 0$. Similar relations, allowing also to determine the creep compliance $J(t)$ [16, 17], are obtained for strain-strain and strain-stress correlations functions.

Outline. The stated key relations eq. (5) and eq. (6) are justified theoretically in sect. II. The static fluctuations are discussed in sect. II A before we address the dynamical correlation functions in sects. II B, II C and II D and the macroscopic linear response in sect. II E. Algorithmic details are given in sect. III where the specific model system considered is introduced in sect. III A. The canonical affine plane shear transformations used in this work are specified in sect. III B, the instantaneous shear stress $\hat{\tau}$ and the instantaneous affine shear-elasticity $\hat{\mu}_{\text{A}}$ in sect. III C. The zero-temperature ground state properties of the two-dimensional elastic network are summarized in sect. III D. Some technical details related to the finite-temperature simulation of the Gaussian λ -ensemble using a Metropolis Monte Carlo (MC) scheme as a function of the maximum strain displacement rate κ , the second key operational parameter of this study, are given in sect. III E. Section IV presents the numerical results obtained by molecular dynamics (MD) simulations at one finite (albeit small) temperature T and one relatively high value of the friction constant ζ of the Langevin thermostat used [1]. The relevant static properties are described in sect. IV A before we turn to the dynamical strain-strain (sect. IV B), strain-stress (sect. IV C) and stress-stress (sect. IV D) correlation functions. Our work is summarized in sect. V.

II. THEORETICAL CONSIDERATIONS

A. Static fluctuations

Lebowitz-Percus-Verlet transform. We begin by restating the LPV transform in a convenient form assuming that the relevant extensive variable is the (rescaled) shear strain $X = V\gamma$ and the conjugated intensive variable the shear stress $I = \tau$. Following Lebowitz *et al.* [1, 2], one verifies (see also sect. II.A of ref. [8]) that to leading order

$$\left\langle \delta \hat{A} \delta \hat{B} \right\rangle \Big|_{\lambda=0} = \left\langle \delta \hat{A} \delta \hat{B} \right\rangle \Big|_{\lambda=1} + \frac{G_{\text{eq}}}{\beta V} \frac{\partial A}{\partial \tau} \frac{\partial B}{\partial \tau} \quad (8)$$

for the transformation of $\langle \delta \hat{A} \delta \hat{B} \rangle$ with $\delta \hat{A} \equiv \hat{A} - \langle \hat{A} \rangle$ and $\delta \hat{B} \equiv \hat{B} - \langle \hat{B} \rangle$ from the NV γ T-ensemble ($\lambda = 1$) to the NV τ T-ensemble ($\lambda = 0$). The more general transformation between arbitrary λ -ensembles can be found by reworking the saddle-point approximation of ref. [2] taking into account that the fluctuations around the peak of the distribution of the extensive variable is now not set by the modulus G_{eq} of the system but by the effective modulus $G_{\text{eff}} = G_{\text{eq}} + G_{\text{ext}}$. How this may be done can be seen in sect. 2.5 of ref. [18] for the volume $X = V$ as extensive variable and the (negative) pressure $I = -P$ as intensive variable. Rewriting the latter result to the present case we get the generalized LPV transform

$$\left\langle \delta \hat{A} \delta \hat{B} \right\rangle \Big|_{\lambda} = \left\langle \delta \hat{A} \delta \hat{B} \right\rangle \Big|_{\lambda=1} + (1 - \lambda) \frac{G_{\text{eq}}}{\beta V} \frac{\partial A}{\partial \tau} \frac{\partial B}{\partial \tau} \quad (9)$$

which reduces for $\lambda = 0$ to eq. (8).

Strain-strain fluctuations. Let us check the ensemble dependence of the rescaled strain-strain fluctuations $\mu_{\gamma\gamma} \equiv \beta V \langle \delta \hat{\gamma}^2 \rangle$ [19]. The generalized Gaussian ensemble corresponds to replacing the shear modulus G_{eq} of the system by the effective modulus $G_{\text{eff}} = G_{\text{eq}} + G_{\text{ext}}$. As already stated above, eq. (4), this leads to [20]

$$\mu_{\gamma\gamma} = 1/G_{\text{eff}} = (1 - \lambda)/G_{\text{eq}}. \quad (10)$$

One verifies readily that the postulated LPV transform for general λ , eq. (9), is consistent with this result. To see this one sets $\mathcal{A} = \mathcal{B} = V\gamma$ and uses the fact that the strain fluctuations must vanish in the NV γ T-ensemble, i.e. that the first term on the right hand-side of eq. (9) must vanish.

Strain-stress fluctuations. Setting $\mathcal{A} = V\gamma$ and $\mathcal{B} = \tau$ and using again that the NV γ T-term in eq. (9) must vanish, it is seen from the LPV transform that the strain-stress fluctuations $\mu_{\gamma\tau} \equiv \beta V \langle \delta \hat{\gamma} \delta \hat{\tau} \rangle$ [19] should scale as

$$\mu_{\gamma\tau} = 1 - \lambda. \quad (11)$$

This result can be also obtained directly by replacing in the definition of $\mu_{\gamma\tau}$ the fluctuation $\delta \hat{\tau}$ by $G_{\text{eq}} \delta \hat{\gamma}$ and using then the strain-strain relation, eq. (10).

Stress-stress fluctuations. We turn to the most important stress-stress fluctuation $\mu_{\tau\tau} \equiv \beta V \langle \delta \hat{\tau}^2 \rangle$ [19]. We set now $\mathcal{A} = \mathcal{B} = \tau$ in the LPV transform. Since the stress fluctuations do *not* vanish in the NV γ T-ensemble the corresponding term must now be included. This yields [20]

$$\mu_{\tau\tau} |_{\lambda} = \mu_{\tau\tau} |_{\lambda=1} + (1 - \lambda) G_{\text{eq}}. \quad (12)$$

Interestingly, the contribution $(1 - \lambda) G_{\text{eq}}$ may be rewritten using the notation $\langle f(\hat{\gamma}) \rangle_{\gamma} \equiv \int d\hat{\gamma} p(\hat{\gamma}; \lambda) f(\hat{\gamma})$ for the strain-average of a property $f(\hat{\gamma})$ with $p(\hat{\gamma}; \lambda)$ being the normalized strain-distribution for the considered λ -ensemble. The total mean stress τ of the ensemble is thus given by $\tau = \langle \tau(\hat{\gamma}) \rangle_{\gamma}$ with $\tau(\hat{\gamma})$ being the average shear-stress of all configurations of shear-strain $\hat{\gamma}$. Using that $p(\hat{\gamma}; \lambda)$ is a Gaussian and that $\delta \tau(\hat{\gamma}) \equiv \tau(\hat{\gamma}) - \tau = G_{\text{eq}}(\hat{\gamma} - \gamma_0)$ with γ_0 being the maximum of the distribution, it is then seen that

$$(1 - \lambda) G_{\text{eq}} = \frac{G_{\text{eq}}^2}{G_{\text{eff}}} = \beta V \langle \delta \tau(\hat{\gamma})^2 \rangle_{\gamma}. \quad (13)$$

Using eq. (12) this implies in turn

$$\mu_{\tau\tau} |_{\lambda} = \mu_{\tau\tau} |_{\lambda=1} + \beta V \langle \delta \tau(\hat{\gamma})^2 \rangle_{\gamma} \quad (14)$$

as one expects to lowest order from a standard saddle-point approximation.

Stress-fluctuation formula for shear modulus. Subtracting the transform for $\lambda = 0$ from eq. (12) confirms the key result eq. (5). As shown in ref. [10], $\mu_{\tau\tau} |_{\lambda=0}$ can be reduced by integration by parts to the affine shear-elasticity μ_A . Since the latter expression is a simple average, i.e. the same value μ_A is obtained in any ensemble, eq. (5) may be further simplified as [20]

$$\mu_{\tau\tau} |_{\lambda} = \mu_A - \lambda G_{\text{eq}}. \quad (15)$$

It is thus sufficient to compute the material constants μ_A and G_{eq} in any ensemble to obtain the stress-stress fluctuations $\mu_{\tau\tau}$ as a function of λ . Note that the special case for $\lambda = 1$ corresponds to the well-known stress-fluctuation formula [4, 8, 21, 22]

$$G_{\text{eq}} = \mu_A - \mu_{\tau\tau} |_{\lambda=1} \quad (16)$$

used in numerous numerical studies to compute the modulus G_{eq} conveniently in the NV γ T-ensemble [8–10, 18, 22–26].

B. Dynamics: Definitions and general relations

Introduction. We define now several dynamical observables of interest, which will be investigated numerically in sect. IV, and remind some well-known general relations [1, 11, 27]. Time translational symmetry ($t \leftrightarrow t + \delta t$) and time reversal symmetry ($t \leftrightarrow -t$) are assumed. We use $\hat{a}(t)$ and $\hat{b}(t)$ for either the instantaneous shear strain $\hat{\gamma}$ or the shear stress $\hat{\tau}$, $a \equiv \langle \hat{a} \rangle$ and $b \equiv \langle \hat{b} \rangle$ for their thermodynamic averages and $\delta \hat{a}(t) \equiv \hat{a}(t) - a$ and $\delta \hat{b}(t) \equiv \hat{b}(t) - b$ for their time-dependent fluctuations.

Mean-square displacements. We define (generalized) mean-square displacements (MSD) by

$$g_{ab}(t) \equiv \frac{\beta V}{2} \left\langle (\hat{a}(t) - \hat{a}(0))(\hat{b}(t) - \hat{b}(0)) \right\rangle \quad (17)$$

where the prefactor $\beta V/2$ has been introduced for convenience [19]. Obviously, $g_{ab}(t) = g_{ba}(t)$, $g_{ab}(t) = g_{ab}(-t)$ as may be seen using the above-mentioned symmetries, $g_{ab}(t) \rightarrow 0$ for $t \rightarrow 0$ and

$$g_{ab}(t) \rightarrow \mu_{ab} \equiv \beta V \left\langle \delta \hat{a} \delta \hat{b} \right\rangle \text{ for } t \gg T_{ab} \quad (18)$$

with T_{ab} being the characteristic time needed to reach this thermodynamic limit [28].

Correlation functions. Similarly, we define dynamic correlation functions by $C_{ab}(t) \equiv \beta V \langle \delta \hat{a}(t) \delta \hat{b}(0) \rangle$ [19]. Obviously, $C_{ab}(0) = \mu_{ab}$, $C_{ab}(t) = C_{ab}(-t)$ and $C_{ab}(t) = C_{ba}(t)$. The latter identity is seen from [3, 11]

$$\left\langle \hat{a}(t) \hat{b}(0) \right\rangle = \left\langle \hat{a}(0) \hat{b}(-t) \right\rangle = \left\langle \hat{b}(t) \hat{a}(0) \right\rangle \quad (19)$$

where the time translational invariance is used in the first step and the time reversal symmetry in the second step. Using again both symmetries one verifies that [11, 27]

$$g_{ab}(t) = C_{ab}(0) - C_{ab}(t) = \mu_{ab} - C_{ab}(t). \quad (20)$$

This implies that $C_{ab}(t) \rightarrow 0$ for large times $t \gg T_{ab}$ [28]. Albeit $g_{ab}(t)$ and $C_{ab}(t)$ thus contain the same information it will be sometimes better for theoretical or numerical reasons to focus on either $g_{ab}(t)$ or $C_{ab}(t)$. Since $g_{ab}(t) \rightarrow 0$ for $t \rightarrow 0$ it will be natural, e.g., to consider the double-logarithmic representation of $g_{ab}(t)$ to clarify the power-law scaling of the correlations at short times.

Finite-time dependence of fluctuation estimation. As defined in sect. II A, μ_{ab} is a thermodynamic ensemble average, hence, a time-independent property. In practice, μ_{ab} may, however, often be estimated using a time series (a_k, b_k) with a finite number n of more or less correlated entries [1, 5]. It is supposed here that these series are sampled with a constant time interval of length δt , i.e. n corresponds to a time $t = (n-1)\delta t$. With $\overline{\mathcal{A}_k} \equiv \frac{1}{n} \sum_{k=1}^n \mathcal{A}_k$ denoting such a finite average, one samples the n -dependent observable [19]

$$\overline{\mu_{ab}(n)} \equiv \beta V \left\langle \overline{(\hat{a}_k - \overline{\hat{a}_k})(\hat{b}_k - \overline{\hat{b}_k})} \right\rangle \quad (21)$$

with $\langle \dots \rangle$ standing for an additional ensemble average over different time series of n subsequent data points. We have $\overline{\mu_{ab}(n)} = 0$ for $n = 1$ and $\overline{\mu_{ab}(n)} \rightarrow \mu_{ab}$ for $n \rightarrow \infty$ in an ergodic system. Interestingly, the detailed time-dependence of $\overline{\mu_{ab}(n)}$ can be obtained from a weighted integral of the correlation function $C_{ab}(t)$ [5, 9]. To see this we note first the identity

$$\overline{(\hat{a}_k - \overline{\hat{a}_k})(\hat{b}_k - \overline{\hat{b}_k})} = \frac{1}{2n^2} \sum_{k,l=1}^n (\hat{a}_k - \hat{a}_l)(\hat{b}_k - \hat{b}_l) \quad (22)$$

which can be verified by straightforward algebra. (See sect. 2.4 of ref. [27].) Using time translational invariance this implies

$$\overline{\mu_{ab}(n)} = \frac{2}{n^2} \sum_{k=1}^n (n-k) g_{ab}(\delta t k) \quad (23)$$

where the weight $(n-k)$ stems from the finite length of the trajectory used. We change now to continuous time variables, $k \rightarrow s = (k-1)\delta t$, and replace the discrete sum by the time integral

$$\overline{\mu_{ab}(t)} = \frac{2}{t} \int_0^t ds (1-s/t) g_{ab}(s). \quad (24)$$

Using eq. (20) this yields the general relation

$$1 - \frac{\overline{\mu_{ab}(t)}}{\mu_{ab}} = \frac{2}{t} \int_0^t ds (1-s/t) \frac{C_{ab}(s)}{C_{ab}(0)} \quad (25)$$

which can be used to obtain $\overline{\mu_{ab}(t)}$ if the correlation function $C_{ab}(t)$ is known.

Relaxation time θ_{ab} . Interestingly, the time integral in eq. (25) must become constant in all cases considered below where $C_{ab}(t)$ vanishes ultimately for $t \rightarrow \infty$. (This applies if a finite shear-barostat is switched on.) Defining the characteristic relaxation time

$$\theta_{ab} \equiv \lim_{t \rightarrow \infty} \int_0^t ds (1-s/t) \frac{C_{ab}(s)}{\mu_{ab}}, \quad (26)$$

this leads to

$$1 - \overline{\mu_{ab}(t)}/\mu_{ab} \rightarrow 2\theta_{ab}/t \text{ for } t \rightarrow \infty \quad (27)$$

as one expects for the Poisson statistics of uncorrelated events [5]. One may thus determine the relaxation time θ_{ab} from the large-time asymptotics of $\overline{\mu_{ab}(t)}$ [29].

C. Dynamics: Additional model assumptions

Let us suppose that the MSD $g_{ab}(t)$ is diffusive for short times, i.e. $g_{ab}(t) = D_{ab}t/2$ for $t \ll T_{ab}$ with D_{ab} being a diffusion constant. Matching this short time regime with $g_{ab}(t) = \mu_{ab}$ for $t \gg T_{ab}$ gives the possibility to operationally *define* T_{ab} as the crossover time

$$T_{ab} \equiv 2\mu_{ab}/D_{ab}. \quad (28)$$

Different short-time dynamics may suggest of course a different operational definition. Let us further assume an exponentially decaying correlation function $C_{ab}(t) = \mu_{ab} \exp(-x)$ with $x = t/T_{ab}$. Using eq. (20) this is seen to be consistent with a diffusive short-time regime and eq. (28). It follows by integration from eq. (25) that

$$1 - \frac{\overline{\mu_{ab}(t)}}{\mu_{ab}} = f_{\text{Debye}}(x) \equiv \frac{2}{x^2} [\exp(-x) - 1 + x] \quad (29)$$

using the Debye function well-known in polymer science [27]. For large reduced times $x \gg 1$ this leads to $1 - \bar{\mu}_{ab}(t)/\mu_{ab} \rightarrow 2T_{ab}/t$, i.e. by comparison with eq. (27) we have $T_{ab} = \theta_{ab}$ for an exponentially decaying correlation function.

As we shall see in sect. IVD, it may also occur that the correlation function is more or less constant between a local (barostat independent time) τ_A up to a (barostat dependent) time τ_* , i.e. essentially $C_{ab}(t) \approx cH(\tau_* - t)$ with c being a constant and $H(x)$ the Heaviside function. It follows from eq. (26) that

$$1 - \frac{\bar{\mu}_{ab}(t)}{\mu_{ab}} \approx \begin{cases} c & \text{for } \tau_A \ll t \ll \tau_* \\ c \tau_*/t & \text{for } \tau_* \ll t, \end{cases} \quad (30)$$

i.e. $\theta_{ab} \approx \tau_* c/2$ to leading order.

D. Dynamics: Ensemble effects

Introduction. We have just stated various general relations applying to all ensembles. These relations do, however, not allow to relate the dynamical correlations between different λ . Since some ensembles are more readily computed than others, it would be useful to have a transformation relation such as the LPV transform for static fluctuations considered in sect. IIA. We emphasize that the correlation functions depend in general on the ensemble, i.e. the parameter λ , and on the dynamics of the shear-barostat. Since in the end we want to describe the intrinsic relaxation dynamics of the system, it is sufficient to focus on the limit where the barostat becomes very slow such that it becomes essentially irrelevant for the system evolution below an upper time τ_* . We consider the limit where this time τ_* is much larger than any intrinsic relaxation time of the system. Since we want still to consider meaningful thermal averages with respect to the chosen ensemble, we need either trajectories of a time interval t_{traj} much larger than τ_* to allow the full sampling of the phase space or, equivalently, we need to average over independent start configurations representing the ensemble. Under these two assumptions useful transformation relations can be formulated by reworking the generalization of the LPV transform for dynamical correlations replacing the system modulus G_{eq} by the effective modulus G_{eff} . Being beyond the scope of this paper, we proceed by postulating the central scaling relation for the MSD $g_{ab}(t)$ and argue briefly why this relation is natural. We discuss then in turn the strain-strain correlations $C_{\gamma\gamma}(t)$, the strain-stress correlations $C_{\gamma\tau}(t)$ and the stress-stress correlations $C_{\tau\tau}(t)$ for different λ . Alternative, more direct ways to derive the relations are mentioned.

Scaling relations. We postulate that under the two assumptions made above the MSD $g_{ab}(t)$ does not depend on the ensemble

$$g_{ab}(t) \sim \lambda^0 \text{ for } t \ll \tau_*(\lambda), \quad (31)$$

i.e. the MSD behaves as a simple mean. This scaling postulate is justified by two facts. Firstly, the barostat is (by construction) too weak to change for $t \ll \tau_*$ the evolution of the system. Secondly, that the starting points of the trajectory at $t = 0$ are distributed according to the considered ensemble must become an irrelevant higher order effect (vanishing rapidly with the system volume V), since the MSD probes displacements with respect to the starting points, not their absolute values. The fundamental scaling, eq. (31), implies using eq. (20) that

$$C_{ab}(t) = \mu_{ab}(\lambda) - g_{ab}(t) \text{ for } t \ll \tau_*(\lambda) \quad (32)$$

where only the first term on the right hand-side depends on λ . This leads us finally to the general transformation relation between correlation functions

$$C_{ab}(t)|_\lambda = C_{ab}(t)|_{\lambda=1} + \mu_{ab}|_\lambda - \mu_{ab}|_{\lambda=1} \quad (33)$$

where $\lambda = 1$ stands for the NV γ T-ensemble with $\gamma = \gamma_{\text{ext}}$. The two static contributions on the right hand-side can be further simplified using results from sect. IIA. This demonstrates the linear relation $\mu_{ab}|_\lambda - \mu_{ab}|_{\lambda=1} \sim 1 - \lambda$.

Strain-strain correlations. Since $\hat{\gamma}(t) \approx \hat{\gamma}(0)$ for $t \ll \tau_*$, the MSD $g_{\gamma\gamma}(t)$ must vanish to leading order. Using eq. (32) this implies [20]

$$C_{\gamma\gamma}(t) = \mu_{\gamma\gamma} = (1 - \lambda)/G_{\text{eq}} \text{ for } t \ll \tau_*(\lambda). \quad (34)$$

This result is directly obtained by setting $\hat{\gamma}(t) = \hat{\gamma}(0)$ in the definition of $C_{\gamma\gamma}(t)$. We emphasize that it is also consistent with the LPV transform, eq. (9), as one verifies by setting $I = \tau$, $X = V\gamma$, $\mathcal{A} = V\gamma(t)$ and $\mathcal{B} = V\gamma(0)$ and using that the strain fluctuation term for $\lambda = 1$ must vanish.

Strain-stress correlations. To determine the strain-stress correlation function $C_{\gamma\tau}(t)$ one may use again that the MSD $g_{\gamma\tau}(t)$ must vanish since $\hat{\gamma}(t) \approx \hat{\gamma}(0)$ for $t \ll \tau_*$. Using eq. (32) this implies [20]

$$C_{\gamma\tau}(t) = \mu_{\gamma\tau} = 1 - \lambda \text{ for } t \ll \tau_*(\lambda). \quad (35)$$

This result is also obtained from the LPV transform setting $\mathcal{A} = V\gamma(t)$ and $\mathcal{B} = \tau(0)$ and using again that $\langle \delta\hat{A}\delta\hat{B} \rangle|_{\lambda=1} = 0$. The postulated scaling eq. (31) has thus led again to a reasonable result.

Stress-stress correlations. Interestingly, as one may see from the NV γ T-ensemble limit considered in [9, 10], the stress-stress MSD $g_{\tau\tau}(t)$ is not expected to simply vanish for $t \ll \tau_*$ as in the two previous cases. (The instantaneous stress $\hat{\tau}$ fluctuates even at a fixed strain $\hat{\gamma}$.) However, eq. (33) still holds leading to [20]

$$C_{\tau\tau}(t)|_\lambda = C_{\tau\tau}(t)|_{\lambda=1} + (1 - \lambda)G_{\text{eq}} \text{ for } t \ll \tau_*(\lambda) \quad (36)$$

where the static term on the right hand-side has been simplified using eq. (5). This confirms the key relation eq. (6) announced in the Introduction. Note that the correlation function $C_{\tau\tau}(t)|_{\lambda=1}$ in the NV γ T-ensemble must vanish beyond some local time scale τ_A which does

depend on the network considered but, of course, not on the shear-barostat. For a sufficiently slow barostat the correlation function thus becomes constant

$$C_{\tau\tau}(t) = (1 - \lambda)G_{\text{eq}} \text{ for } \tau_A \ll t \ll \tau_*(\lambda) \quad (37)$$

where we have dropped $|\lambda$. Using eq. (32) this leads to the remarkable relation

$$g_{\tau\tau}(t) = \mu_A - G_{\text{eq}} \text{ for } \tau_A \ll t \ll \tau_*(\lambda) \quad (38)$$

which must hold for all $\lambda \leq 1$. We note finally that while for $\lambda < 1$ the MSD $g_{\tau\tau}(t) \rightarrow \mu_{\tau\tau}$ for $t \gg \tau_*$, $g_{\tau\tau}(t) = \mu_A - G_{\text{eq}}$ holds for all times $t \gg \tau_A$ for $\lambda = 1$ according to stress-fluctuation formula, eq. (16).

E. Dynamics: Macroscopic linear response

Introduction. The experimentally important macroscopic linear response measured by the creep compliance $J(t)$ and the shear relaxation modulus $G(t)$ [16, 17, 27] may be obtained conveniently in an equilibrium simulation at a given λ using some of the correlation functions discussed above. Please note that being material properties of the given state point (experimentally obtained using a simple average, not a fluctuation) both response functions $J(t)$ and $G(t)$ do, of course, not depend on λ .

Creep compliance. Let us first consider the creep compliance $J(t) \equiv \langle \delta\hat{\gamma}(t) \rangle / \delta\tau_{\text{ext}}$ for $t \geq 0$. It is assumed that for $t < 0$ the system is at thermal equilibrium and the internal mean stress τ equals the applied external stress τ_{ext} of the NV τ T-ensemble. After imposing at $t = 0$ a small increment $\delta\tau_{\text{ext}}$, the creep compliance $J(t)$ measures the ensuing average strain increment $\langle \delta\hat{\gamma}(t) \rangle$. We note *en passant* that the average internal shear stress $\langle \hat{\tau}(t) \rangle$ does neither immediately reach the new equilibrium value $\tau_{\text{ext}} + \delta\tau_{\text{ext}}$ but shows a similar time dependence as the strain. Reworking the arguments put forward by Doi and Edwards, see eq. (3.67) of ref. [27], it is seen that

$$J(t) = g_{\gamma\gamma}(t)|_{\lambda=0} \text{ for } |\delta\tau_{\text{ext}}| \ll 1, \quad (39)$$

i.e. the creep compliance is most readily computed using the strain-strain MSD $g_{\gamma\gamma}(t)$ in the NV τ T-ensemble. As described in sect. III E, we shall change the shear-strain $\hat{\gamma}(t)$ using a MC shear-barostat which corresponds to a perfectly viscous dynamics. One thus expects $C_{\gamma\gamma}(t) = \mu_{\gamma\gamma} \exp(-t/T_{\gamma\gamma})$ for the strain-strain correlations. Using $\mu_{\gamma\gamma} = 1/G_{\text{eq}}$ for $\lambda = 0$ and eq. (20) this suggest

$$J(t) = \frac{1}{G_{\text{eq}}} [1 - \exp(-t/T_{\gamma\gamma})] \quad (40)$$

in agreement with the Kelvin-Voigt model [17] representing a purely viscous damper and a purely elastic spring connected in parallel.

Shear relaxation modulus. The shear relaxation modulus $G(t) \equiv \langle \delta\hat{\tau}(t) \rangle / \delta\gamma$ may be obtained from the stress increment $\langle \delta\hat{\tau}(t) \rangle$ for $t > 0$ after a small step strain with $|\delta\gamma| \ll 1$ has been imposed at time $t = 0$. It is well known that the components of the Fourier transformed relaxation modulus $G(t)$, the storage modulus $G'(\omega)$ and the loss modulus $G''(\omega)$, are directly measurable in an oscillatory shear strain experiment [10, 17]. As seen, e.g., by eq. (32) in ref. [10], it can be demonstrated by integration by parts that

$$G(t) = C_{\tau\tau}(t)|_{\lambda=0} \text{ for } t \ll \tau_*(\lambda = 0), \quad (41)$$

i.e. the barostat should be irrelevant on the time scales considered. Using the transformation relation between different ensembles, eq. (36), the relaxation modulus may equivalently be obtained for other λ according to

$$G(t) = C_{\tau\tau}(t)|_{\lambda} + \lambda G_{\text{eq}} \text{ for } t \ll \tau_*(\lambda). \quad (42)$$

Since for large times $G(t) \rightarrow G_{\text{eq}}$, this implies $C_{\tau\tau}(t)|_{\lambda} \rightarrow (1 - \lambda)G_{\text{eq}}$ consistently with eq. (37). For the specific case $\lambda = 1$ eq. (42) yields

$$G(t) = C_{\tau\tau}(t)|_{\lambda=1} + G_{\text{eq}} \quad (43)$$

which holds for all times t since the barostat becomes irrelevant for $\lambda \rightarrow 1$. Note that eq. (43) may also be derived directly (without using the transformation relation between different ensembles) using Boltzmann's superposition principle for an arbitrary strain history and the standard fluctuation-dissipation theorem for the after-effect function [11] as shown elsewhere [9, 10]. Two immediate consequences of eq. (43) are (i) that $G(t)$ only becomes equivalent to $C_{\tau\tau}(t)|_{\lambda=1}$ for $t > 0$ in the liquid limit where (trivially) $G_{\text{eq}} = 0$ and (ii) that the shear modulus G_{eq} is only probed by $G(t)$ on time scales $t \gg \tau_A$ where $C_{\tau\tau}(t)|_{\lambda=1}$ must vanish. In principle, it is thus *impossible* to obtain the static shear modulus G_{eq} of an elastic body only from $C_{\tau\tau}(t)|_{\lambda=1}$ as often incorrectly assumed [26, 30].

III. ALGORITHMIC DETAILS

A. Model Hamiltonian

To illustrate our key relations we present in sect. IV numerical data obtained using a periodic two-dimensional ($d = 2$) network of N_l harmonic springs connecting N vertices. The model Hamiltonian is given by the sum $\hat{\mathcal{H}} = \hat{\mathcal{H}}_{\text{id}} + \hat{\mathcal{H}}_{\text{ex}}$ of a kinetic energy contribution

$$\hat{\mathcal{H}}_{\text{id}} = \frac{m}{2} \sum_{i=1}^N v_i^2, \quad (44)$$

with v_i being the velocity of vertex i and m its (assumed) monodisperse mass, and an excess potential

$$\hat{\mathcal{H}}_{\text{ex}} = \sum_{l=1}^{N_l} u_l(r_l) \text{ with } u_l(r) = \frac{1}{2} K_l (r - R_l)^2 \quad (45)$$

where K_l denotes the spring constant, R_l the reference length and $r_l = |\underline{r}_i - \underline{r}_j|$ the length of spring l . The sum runs over all springs l connecting pairs of beads i and j with $i < j$ at positions \underline{r}_i and \underline{r}_j . The vertex mass m and Boltzmann's constant k_B are set to unity and Lennard-Jones (LJ) units [1] are assumed.

B. Canonical affine shear transformations

While the box volume V is kept constant throughout this work, we shall frequently change the shape of the simulation box. As sketched in panel (a) of fig. 1, we perform plane shear transformations of the instantaneous shear strain $\hat{\gamma} \rightarrow \hat{\gamma} + \delta\gamma$ with an essentially infinitesimal strain increment $\delta\gamma$. We assume that not only the box shape is changed but that the particle positions \underline{r} (using the principal box convention [1]) follow the imposed macroscopic constraint in an *affine* manner according to

$$r_x \rightarrow r_x + \delta\gamma r_y \quad \text{for } |\delta\gamma| \ll 1 \quad (46)$$

with all other coordinates remaining unchanged. Albeit not strictly necessary for the demonstration of our key relations, we assume, moreover, that this shear transformation is also *canonical* [4, 31]. This implies that the x -component of the velocity must transform as [10]

$$v_x \rightarrow v_x - \delta\gamma v_y \quad \text{with } |\delta\gamma| \ll 1. \quad (47)$$

We emphasize the negative sign in eq. (47) which assures that Liouville's theorem is obeyed [10, 31].

C. Shear stress and affine shear-elasticity

Let $\hat{\mathcal{H}}(\delta\gamma) = \hat{\mathcal{H}}_{\text{id}}(\delta\gamma) + \hat{\mathcal{H}}_{\text{ex}}(\delta\gamma)$ denote the system Hamiltonian of a configuration originally at $\hat{\gamma}$ strained using a canonical affine transformation to $\hat{\gamma} + \delta\gamma$ compactly written as a function of the strain increment $\delta\gamma$. The instantaneous shear stress $\hat{\tau}$ and the instantaneous affine shear-elasticity $\hat{\mu}_A$ may be defined as the expansion coefficients associated to the energy change

$$\delta\hat{\mathcal{H}}(\delta\gamma)/V = \hat{\tau}\delta\gamma + \hat{\mu}_A\delta\gamma^2/2 \quad \text{for } |\delta\gamma| \ll 1 \quad (48)$$

with $\hat{\gamma}$ being the reference, i.e. [32]

$$\hat{\tau} \equiv \hat{\mathcal{H}}'(\delta\gamma)/V|_{\hat{\gamma}} \quad \text{and} \quad (49)$$

$$\hat{\mu}_A \equiv \hat{\mathcal{H}}''(\delta\gamma)/V|_{\hat{\gamma}}. \quad (50)$$

The derivatives $\hat{\mathcal{H}}'(\delta\gamma)$ and $\hat{\mathcal{H}}''(\delta\gamma)$ with respect to $\delta\gamma$ may be computed as shown in sect. 2.1 of [10]. Similar relations apply for the corresponding contributions $\hat{\tau}_{\text{id}}$ and $\hat{\tau}_{\text{ex}}$ to $\hat{\tau} = \hat{\tau}_{\text{id}} + \hat{\tau}_{\text{ex}}$ and for the contributions $\hat{\mu}_{A,\text{id}}$ and $\hat{\mu}_{A,\text{ex}}$ to $\hat{\mu}_A = \hat{\mu}_{A,\text{id}} + \hat{\mu}_{A,\text{ex}}$. Using eq. (44) this

implies [10]

$$\hat{\tau}_{\text{id}} = -\frac{1}{V} \sum_{i=1}^N m_i v_{i,x} v_{i,y} \quad \text{and} \quad (51)$$

$$\hat{\mu}_{A,\text{id}} = \frac{1}{V} \sum_{i=1}^N m_i v_{i,y}^2 \quad (52)$$

for the ideal contributions to the shear stress and the affine shear-elasticity. Note that the minus sign for the shear stress is due to the minus sign in eq. (47) required for a canonical transformation. For the excess contributions one obtains [10]

$$\hat{\tau}_{\text{ex}} = \frac{1}{V} \sum_l r_l u'(r_l) n_{l,x} n_{l,y} \quad \text{and} \quad (53)$$

$$\begin{aligned} \hat{\mu}_{A,\text{ex}} &= \frac{1}{V} \sum_l (r_l^2 u''(r_l) - r_l u'(r_l)) n_{l,x}^2 n_{l,y}^2 \\ &+ \frac{1}{V} \sum_l r_l u'(r_l) n_{l,y}^2 \end{aligned} \quad (54)$$

with $\underline{n}_l = \underline{r}_l/r_l$ being the normalized distance vector $\underline{r} = \underline{r}_j - \underline{r}_i$ between the particles i and j . Interestingly, eq. (53) is strictly identical to the corresponding off-diagonal term of the Kirkwood stress tensor [1]. The last term in eq. (54) automatically takes into account the finite normal pressure of the system.

D. Groundstate characterization

Specific network. As explained elsewhere [8, 10], the specific elastic network used in this work has been constructed using the dynamical matrix of a quenched poly-disperse LJ bead glass, i.e. at low temperatures our network has exactly the same mechanical and vibrational properties as the original discrete particle system. Prior to forming the network the bead system was cooled down to $T = 0$ using a constant quenching rate and imposing a normal pressure $P = 2$. The original LJ beads are represented in the snapshot shown in fig. 2 by grey poly-disperse circles, the permanent spring network created from the quenched bead system by lines between vertices. The dark (black) lines indicate repulsive forces between the vertices, while the light (red) lines represent tensile forces. The line width is proportional to the tension (repulsion). Note that the force network is strongly inhomogeneous with zones of weak attractive links embedded within a strong repulsive skeleton as already discussed in refs. [24, 25]. Only a small subvolume of the network is represented. The total periodic box of linear length $L \approx 102.3$ contains $N = 10^4$ vertices and $N_l = 9956$ springs. The monomer density ρ is close to unity.

Finite shear stress τ_0 . Due to the construction of the network the total force acting on each vertex of the reference network must vanish at $T = 0$. As seen in the snapshot, this does not imply that the repulsive and/or

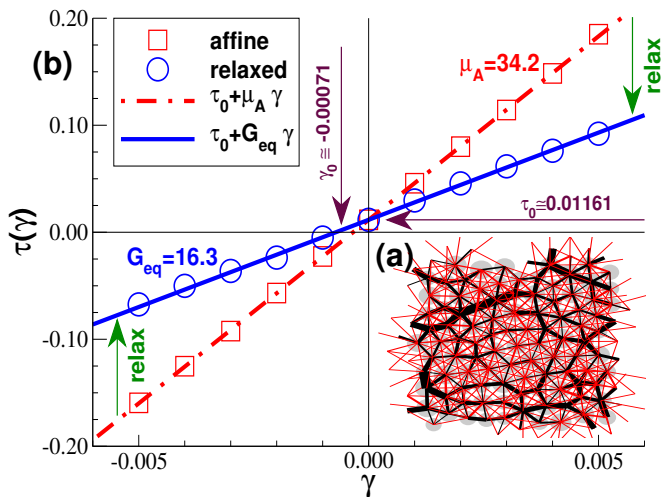


FIG. 2: Groundstate of elastic network model considered in this work assuming eq. (45): (a) Snapshot of a small subvolume of linear length 10 containing about 100 vertices. The lines represent the quenched forces of the athermal ($T = 0$) reference configuration. (b) Shear stress $\tau(\gamma)$ assuming an affine strain (squares) and after energy minimization (circles). In agreement with ref. [10] we find in the first case $\tau(\gamma) = \tau_0 + \mu_A \gamma$ with $\mu_A = 34.2$ (dashed line) and in the second case $\tau(\gamma) = \tau_0 + G_{\text{eq}} \gamma$ with $G_{\text{eq}} = 16.3$ (bold solid line). The stress does not vanish at $\gamma = 0$ where $\tau = \tau_0 = 0.01161$ (horizontal arrow) but at $\gamma = \gamma_0 = -0.00071$ (vertical arrow).

tensile forces transmitted along the springs must also vanish. Due to the periodic boundary conditions and the constant-strain constraint ($\gamma = 0$) the shear stress τ does not necessarily vanish. For a pair potential such as eq. (45) the relevant excess contribution $\hat{\tau}_{\text{ex}}$ of the shear stress is readily computed using the Kirkwood expression, eq. (53). As shown in the main panel of fig. 2 (horizontal arrow), it turns out that for the specific network we use throughout this work we have a finite shear stress $\tau_0 \equiv \tau(\gamma = 0) = 0.01161$.

Affine shear-elasticity μ_A . Let us consider a small affine shear strain according to eq. (46). As shown in panel (b) of fig. 2, one may now compute using eq. (53) the shear stress $\tau(\gamma)$ for different γ (squares). As one expects from the definition of the affine shear-elasticity coefficient μ_A , eq. (48), this yields the linear relation $\tau(\gamma) = \tau_0 + \mu_A \gamma$ with $\mu_A \approx 34.2$ as indicated by the dashed line. The same coefficient μ_A is also obtained directly from the unstrained configuration using eq. (54).

Equilibrium shear modulus G_{eq} . The forces f_i acting on the vertices i of an *affinely* strained network do not vanish in general and the system is normally *not* at mechanical equilibrium. As described elsewhere [10, 25], we relax these forces by first applying a steepest descent algorithm, i.e. by imposing displacements proportional to the force, and then by means of the conjugate gradient method [6]. The ensuing non-affine displacements of the vertices decrease the energy [10] and the magnitude of

the shear stress $\tau(\gamma)$ as may be seen from the large circles indicated in fig. 2. As indicated by the bold solid line these final stresses $\tau(\gamma)$ scale again linearly as

$$\tau(\gamma) = \tau_0 + G_{\text{eq}} \gamma = G_{\text{eq}} (\gamma - \gamma_0) \quad (55)$$

with $G_{\text{eq}} \approx 16.3$ and $\gamma_0 = -\tau_0/G_{\text{eq}} \approx -0.00072$. The affine coefficient μ_A has thus been replaced by the much smaller equilibrium shear modulus G_{eq} of the ground-state network. Note that shear stress vanishes at a strain $\gamma = \gamma_0$ as indicated by the vertical arrow. If the strain γ is allowed to change freely (e.g., using a steepest descent scheme) without any external force τ_{ext} applied, the system relaxes to $\gamma = \gamma_0$.

E. Finite temperature simulations

Molecular dynamics scheme. As discussed in sect. IV, this network is investigated numerically basically by means of a molecular dynamics (MD) simulation [1, 4] at constant particle number $N = 10^4$, box volume $V \approx 102.3^2$ and a small, but finite mean temperature $T = 0.001$. Newton's equations are integrated using a velocity-Verlet algorithm with a tiny time step $\delta t_{\text{MD}} = 10^{-4}$. The temperature T is fixed using a Langevin thermostat with a relatively large friction constant $\zeta = 1$. This was done to suppress artificial long-range correlations in the two-dimensional periodic simulation box.

Thermal averages. Using the measured instantaneous shear stress $\hat{\tau}$ and affine shear-elasticity $\hat{\mu}_A$ we compute, e.g., the thermal averages $\tau \equiv \langle \hat{\tau} \rangle$, $\mu_{\tau\tau} \equiv \beta V \langle \delta \hat{\tau}^2 \rangle$ and $\mu_A \equiv \langle \hat{\mu}_A \rangle$. It can be shown for the respective ideal contributions that [10]

$$\tau_{\text{id}} = \mu_{\tau\tau, \text{id}} = \mu_{A, \text{id}} = P_{\text{id}} = T \rho \quad (56)$$

with P_{id} being the ideal normal pressure contribution. This holds irrespective of the considered λ -ensemble. The ideal contributions are thus negligible. Due to the equivalence of the different axes it is also seen for the excess contributions that [10]

$$\begin{aligned} \mu_{A, \text{ex}} &= \mu_B - P_{\text{ex}} \text{ with} \\ \mu_B &= \frac{1}{V} \sum_l \langle (r_l^2 u''(r_l) - r_l u'(r_l)) n_{l,x}^2 n_{l,y}^2 \rangle \end{aligned} \quad (57)$$

being the Born-Lamé coefficient [7, 22–25, 33] and P_{ex} the excess part of the normal pressure $P = P_{\text{id}} + P_{\text{ex}}$.

Monte Carlo shear-barostat. The MD algorithm for the particles is coupled for $\lambda < 1$ with a Monte Carlo (MC) scheme [1, 5] attempting every MD time step a canonical affine strain increment $\hat{\gamma} \rightarrow \hat{\gamma} + \delta\gamma$ (sect. III B). First, a strain increment $\delta\gamma$ is randomly chosen from a uniformly distributed interval $[-\delta\gamma_{\text{max}}, \delta\gamma_{\text{max}}]$. In order to determine the Metropolis weight [5] we compute next the energy change $\delta\hat{\mathcal{H}} = \hat{\mathcal{H}}(\hat{\gamma} + \delta\gamma) - \hat{\mathcal{H}}(\hat{\gamma})$ of the network which comprises both an excess contribution due to eq. (46) and an ideal contribution due to

G_{ext}	λ	$\mu_{\gamma\gamma}$	$\mu_{\tau\tau}$	A	η	$T_{\gamma\gamma}$	$T_{\gamma\tau}$	$\theta_{\tau\tau}$
-10	-1.59	0.159	60.1	0.997	0.0081	9.2	4.3	13
-6	-0.58	0.097	43.7	0.996	0.0103	5.6	2.7	6
-3	-0.23	0.075	37.9	0.996	0.0117	4.3	2.1	4
0	0	0.061	34.2	0.996	0.0130	3.5	1.7	2
16.3	0.50	0.031	26.1	0.994	0.0184	1.8	0.85	1
100	0.86	0.009	20.1	0.993	0.0348	0.5	0.24	0.3
1000	0.98	0.001	18.1	0.979	0.1030	0.06	0.03	0.3
10000	0.998	-	17.9	0.935	0.3233	0.007	0.003	0.4

TABLE I: Summary of some properties as a function of the external spring constant G_{ext} : $\lambda = G_{\text{ext}}/(G_{\text{eq}} + G_{\text{ext}})$ with $G_{\text{eq}} = 16.3$, strain-strain fluctuation $\mu_{\gamma\gamma}$ (fig. 5), stress-stress fluctuation $\mu_{\tau\tau}$ (fig. 7), acceptance rate A of MC shear-barostat (fig. 3), $\eta(\lambda, \kappa)$ -parameter defined by eq. (61), strain-strain crossover time $T_{\gamma\gamma} \approx \theta_{\gamma\gamma}$ (fig. 8), strain-stress crossover time $T_{\gamma\tau} \approx \theta_{\gamma\tau}$ (fig. 10), stress-stress relaxation time $\theta_{\tau\tau}$ (fig. 15). The dynamical properties (columns 5-9) are only given for $\kappa = 10^{-2}$. The time scales $T_{\gamma\gamma}$, $T_{\gamma\tau}$ and $\theta_{\tau\tau}$ should be compared to the intrinsic relaxation time $\tau_A \approx 0.13$ of the stress-stress correlations for $\kappa \rightarrow 0$ (fig. 11).

eq. (47). Since our system is subjected to an external field $U_{\text{ext}}(\hat{\gamma})$, eq. (3), this gives rise to an additional contribution $\delta U_{\text{ext}} = U_{\text{ext}}(\hat{\gamma} + \delta\gamma) - U_{\text{ext}}(\hat{\gamma})$. The suggested strain move $\delta\gamma$ is accepted if

$$\xi \leq \exp[-\beta(\delta\hat{\mathcal{H}} + \delta U_{\text{ext}})] \quad (58)$$

with ξ being a uniformly distributed random variable with $0 \leq \xi < 1$ [5].

Operational parameters λ and κ . We assume for the external field $U_{\text{ext}}(\hat{\gamma})$ that $\tau_{\text{ext}} \equiv 0$ and $\gamma_{\text{ext}} \equiv \gamma_0$, i.e. the average shear stress τ is imposed to vanish for all ensembles studied and all ensembles compare the same thermodynamic state point. (This was explicitly checked.) The only remaining operational parameter from the static point of view is the external spring constant G_{ext} or, equivalently, $\lambda \equiv G_{\text{ext}}/(G_{\text{eq}} + G_{\text{ext}})$ as sketched in panel (c) of fig. 1. As seen in table I or fig. 3, we vary G_{ext} from -10 , i.e. $\lambda \approx -1.59$, over $G_{\text{ext}} = \lambda = 0$ (NV τ T-ensemble) up to $G_{\text{ext}} = 10000$, i.e. $\lambda \approx 0.998$. The latter case is essentially equivalent to the standard NV γ T-ensemble, i.e. the strain fluctuations become irrelevant for most properties. The second operational parameter of this study is the maximum attempted strain displacement $\delta\gamma_{\text{max}}$ which determines the impact of the shear-barostat on the relaxation dynamics. Since the Metropolis MC move for the strain is performed every MD time step of length δt_{MD} , it is convenient to use instead of $\delta\gamma_{\text{max}}$ the maximum strain increment *rate* $\kappa \equiv \delta\gamma_{\text{max}}/\delta t_{\text{MD}}$. (Since all simulations are performed with the same δt_{MD} , $\delta\gamma_{\text{max}}$ and κ are strictly equivalent.) We compare below the dynamical strain and stress correlations for the five rates $\kappa = 1, 10^{-1}, 10^{-2}, 10^{-3}$ and 10^{-4} for a broad range of λ . For $\lambda = 0.5$ we have computed in addition the values $\kappa = 3, 0.3, 0.03, 0.003$ and

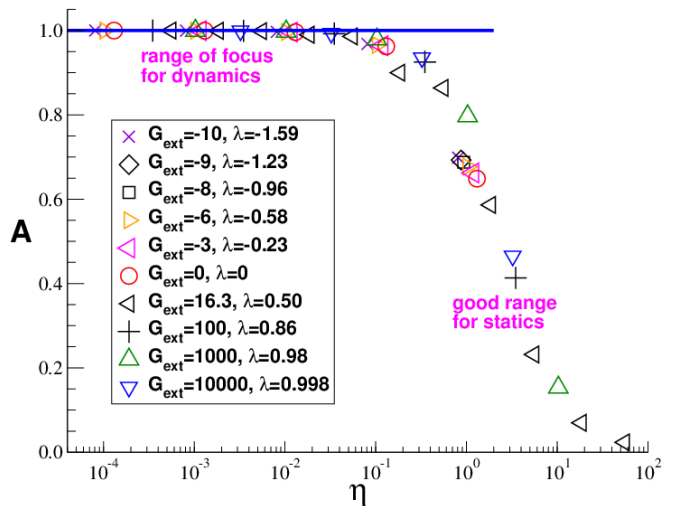


FIG. 3: Acceptance rate A of the Metropolis MC shear-barostat, eq. (58), for a large range of λ and κ as a function of the scaling variable $\eta(\lambda, \kappa)$ as defined by eq. (61).

0.0003. Some properties for $\kappa = 10^{-2}$ are summarized in the columns 5-9 of table I. The simulations become increasingly time consuming with decreasing κ and data obtained for $\kappa = 10^{-4}$ have to be taken with care.

Free strain diffusion limit. The impact of κ can be best judged from the simple limit where neither the system nor the external field restricts the barostat. This is the case for sufficiently small κ depending on λ . In this limit one expects the free diffusion of the strain $\hat{\gamma}(t)$, i.e. $g_{\gamma\gamma}(t) = D_{\gamma\gamma}t/2$ for $t \ll T_{\gamma\gamma}$. Since the (attempted and accepted) strain increment $\delta\gamma$ is uniformly distributed in $[-\delta\gamma_{\text{max}}, \delta\gamma_{\text{max}}]$, we have a mean-square strain step $\langle \delta\gamma^2 \rangle = \delta\gamma_{\text{max}}^2/3$ every δt_{MD} . This implies a diffusion constant

$$D_{\gamma\gamma} = \frac{\beta V}{3} \frac{\delta\gamma_{\text{max}}^2}{\delta t_{\text{MD}}} \sim \kappa^2 \quad (59)$$

in the free-diffusion limit. Using eq. (28) and eq. (4) this yields in turn the corresponding crossover time

$$T_{\gamma\gamma} = 6 \frac{\mu_{\gamma\gamma}}{\beta V} \frac{\delta t_{\text{MD}}}{\delta\gamma_{\text{max}}^2} = 6 \delta t_{\text{MD}}/\eta^2 \quad (60)$$

where we have defined the dimensionless variable

$$\eta(\lambda, \kappa) \equiv \sqrt{\beta V \delta\gamma_{\text{max}}^2 / \mu_{\gamma\gamma}} = \frac{\kappa \delta t_{\text{MD}}}{\sqrt{\langle \delta\hat{\gamma}^2 \rangle}}. \quad (61)$$

Since G_{eq} and δt_{MD} are kept constant in all our simulations, the parameter η determines the dynamical regime for a system of operational parameters λ and κ . As seen in fig. 3 using η as a scaling variable the acceptance rate A of the MC shear-barostat of a broad range of λ and κ can be brought to collapse. For $1 \ll \eta \ll 10$ the MC barostat is most efficient for static properties. For dynamical properties we shall focus below on κ -values where $\eta \ll 0.1$ and thus $A \approx 1$ as emphasized by the solid horizontal line.

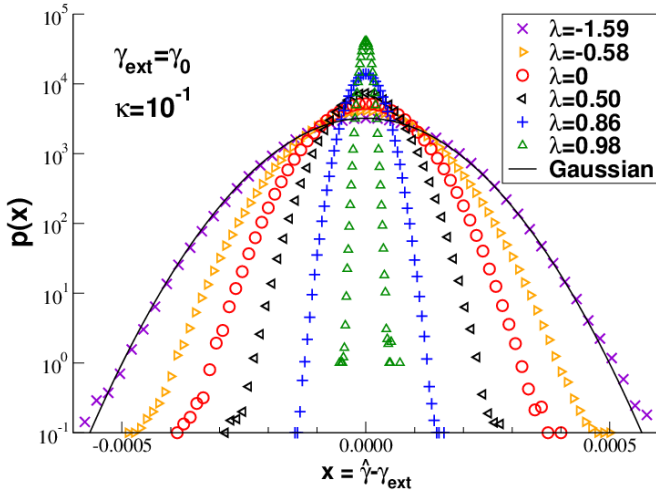


FIG. 4: Normalized histogram $p(x)$ of $x = \hat{\gamma} - \gamma_{\text{ext}}$ for different λ . The line indicates for $\lambda = -1.59$ ($G_{\text{ext}} = -10$) a Gaussian with $\langle \delta \hat{\gamma}^2 \rangle = 1/\beta V G_{\text{eff}} \approx 0.00012^2$.

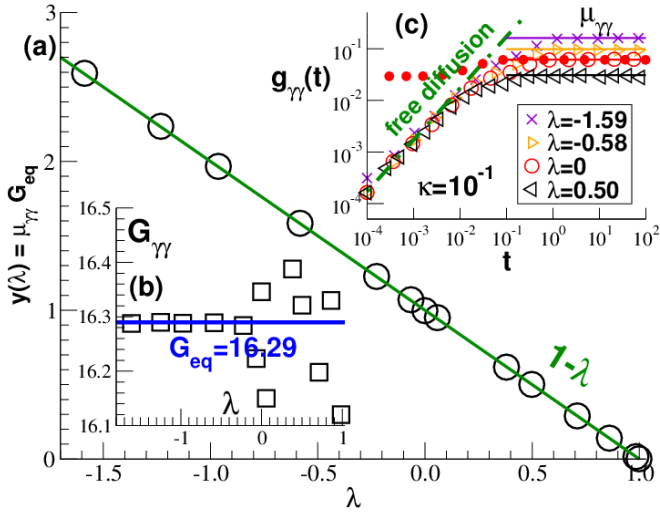


FIG. 5: Second moment of strain fluctuations: (a) Dimensionless $y = \mu_{\gamma\gamma} G_{\text{eq}}$ with $G_{\text{eq}} \equiv 16.3$ as a function of λ showing the linear decay (bold line) expected from eq. (4). (b) Shear modulus $G_{\gamma\gamma}$, eq. (62), confirming $G_{\text{eq}} \approx 16.3$ (bold line). (c) MSD $g_{\gamma\gamma}(t)$ vs. time t for several λ and $\kappa = 10^{-1}$. The dash-dotted line indicates the free-diffusion limit, eq. (59), for short times, the horizontal lines the long-time limit $\mu_{\gamma\gamma}$ for each λ . Also indicated is for $\lambda = 0$ and $\kappa = 1$ (filled circles) an example with $\eta \gg 0.1$ where the initial diffusive regime is suppressed.

IV. COMPUTATIONAL RESULTS

A. Static properties

Strain-strain fluctuations. The equilibrium fluctuations of the strain $\hat{\gamma}$ at a finite temperature $T = 0.001$ for different values of G_{ext} or, equivalently, $\lambda = G_{\text{ext}}/(G_{\text{eq}} + G_{\text{ext}})$ with $G_{\text{eq}} \equiv 16.3$ are presented in fig. 4 and fig. 5.

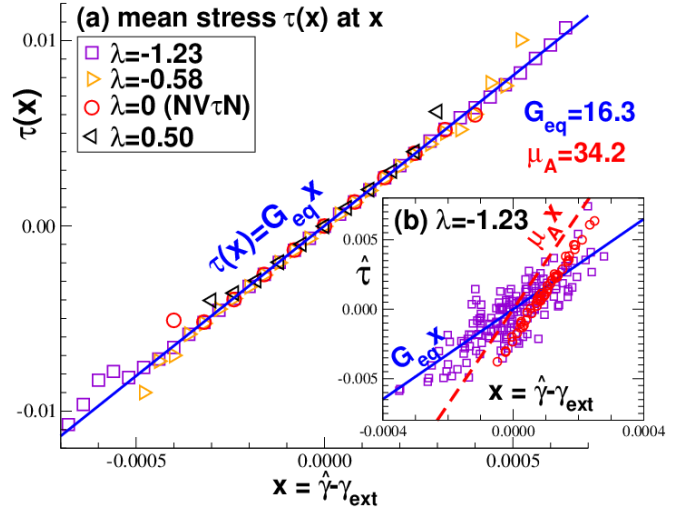


FIG. 6: Strain-stress correlations: (a) Pre-averaged shear stress $\tau(x)$ as a function of $x = \hat{\gamma} - \gamma_{\text{ext}}$. All data collapse on the linear slope with $G_{\text{eq}} = 16.3$ (bold solid line). (b) Scatter plot of 100 data points $(\hat{\gamma}, \hat{\tau})$ for $\lambda = -1.23$ ($G_{\text{ext}} = -9$) with circles corresponding to a tiny time interval $\delta t = 10^{-4}$ (dashed line) and squares to a large $\delta t = 10^{+2}$ (bold solid line) between subsequent configurations.

The given data refer to a maximum strain rate $\kappa = 10^{-1}$ for the Metropolis MC step $\hat{\gamma} \rightarrow \hat{\gamma} + \delta\gamma$ attempted after each MD time step of $\delta t_{\text{MD}} = 10^{-4}$ (sect. III E). That this leads indeed to the desired Gaussian distributions can be seen from fig. 4 where the normalized histogram $p(x)$ is plotted as a function of $x = \hat{\gamma} - \gamma_{\text{ext}}$ with $\gamma_{\text{ext}} = \gamma_0$. As one expects, $p(x) \rightarrow \delta(x)$ for $\lambda \rightarrow 1$. The rescaled second moment $\mu_{\gamma\gamma} \equiv \beta V \langle \delta \hat{\gamma}^2 \rangle$ of the distribution is further analyzed in fig. 5. As one may see from panel (a), $y(\lambda) \equiv \mu_{\gamma\gamma} G_{\text{eq}}$ decreases linearly with λ (bold solid line) and vanishes for $\lambda = 1$ as it should according to eq. (10). In turn this implies that one may determine G_{eq} from

$$G_{\gamma\gamma} \equiv 1/\mu_{\gamma\gamma} - G_{\text{ext}}. \quad (62)$$

As can be seen from panel (b) of fig. 5, using this relation one confirms that the groundstate value $G_{\text{eq}} \approx 16.3$ remains unchanged at a finite temperature $T \ll 1$. The accurate determination of $G_{\gamma\gamma}$ becomes of course more delicate with increasing λ since the MC acceptance rate becomes eventually too small. The data quality in this limit can be readily improved (not shown) by either increasing the sampling time t_{traj} or by decreasing $\kappa \sim \eta$. (The sampling becomes again inefficient if η gets too small.)

Strain-stress correlations. Since the shear modulus G_{eq} is finite, this implies that shear strain and shear stress fluctuations must be correlated [8]. These correlations are addressed in fig. 6. The main panel presents the pre-averaged stress $\tau(x)$ for an instantaneous strain $x = \hat{\gamma} - \gamma_{\text{ext}}$ for several λ [34]. Irrespective of x or λ all data collapse on the linear slope indicated by the bold line with $G_{\text{eq}} = 16.3$. Naturally, it follows from fig. 4 that the statistics must strongly decrease for $x^2 \gg$

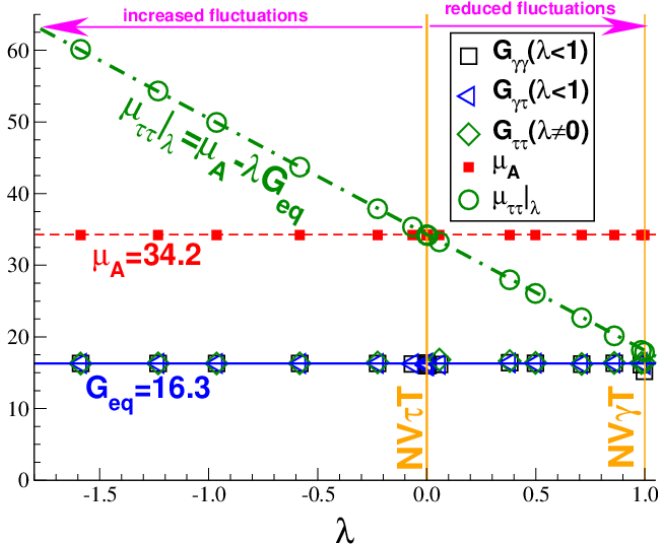


FIG. 7: Determination of shear modulus $G_{\text{eq}} \approx 16.3$ (bold solid line) using $G_{\gamma\gamma}$ for $\lambda < 1$, $G_{\gamma\tau}$ for $\lambda < 1$ and $G_{\tau\tau}$ for $\lambda \neq 0$. Also indicated are the affine shear-elasticity $\mu_A(\lambda) \approx 34.2$ (dashed line) and the stress-stress fluctuation $\mu_{\tau\tau}$ which is seen to decay linearly (bold dash-dotted line) according to eq. (5) down to $\mu_{\tau\tau}|_{\lambda=1} \approx 18$.

$\mu_{\gamma\tau} \equiv \beta V \langle \delta\hat{\gamma} \delta\hat{\tau} \rangle$, i.e. a larger linear-slope window is visible in fig. 6 for smaller λ . Panel (b) of fig. 6 presents two scatter plots of $(\hat{\gamma}, \hat{\tau})$ for $\lambda = -1.23$ ($G_{\text{ext}} = -9$). The small circles correspond to a time series of 100 subsequent and, hence, strongly correlated configurations with $\delta t = \delta t_{\text{MD}}$. On these time scales the configuration has no time to relax the affine displacements imposed by the shear-barostat. As emphasized by the dashed slope this leads to a linear stress-strain relation with a coefficient $\mu_A = 34.2$. Other short-time sequences yield similar, but horizontally shifted linear slopes (not shown). A δt -independent representation of the static strain-stress correlations for large times is obtained if $(\hat{\gamma}, \hat{\tau})$ is indicated for 100 configurations with a time interval $\delta t = 10^2$ (squares). The scatter plot of the latter data is already in nice agreement with a coefficient $G_{\text{eq}} = 16.3$ (bold line). Sampling over *all* data tuples $(\hat{\gamma}, \hat{\tau})$ of a given λ -ensemble one verifies that the shear modulus G_{eq} is accurately determined using the linear regression coefficient

$$G_{\gamma\tau} \equiv \frac{\langle \delta\hat{\gamma} \delta\hat{\tau} \rangle}{\langle \delta\hat{\gamma}^2 \rangle} = \frac{\mu_{\gamma\tau}}{\mu_{\gamma\gamma}} \text{ for } \lambda < 1. \quad (63)$$

Since, as shown in sect. II A, $\mu_{\gamma\gamma} = (1 - \lambda)/G_{\text{eq}}$ and $\mu_{\gamma\tau} = 1 - \lambda$, this ratio must yield G_{eq} for all $\lambda < 1$. Confirming $G_{\text{eq}} = 16.3$ the values of $G_{\gamma\tau}$ for different λ are identical to $G_{\gamma\gamma}$ as shown in fig. 7.

Stress-stress fluctuations. The stress-stress fluctuations $\mu_{\tau\tau} \equiv \beta V \langle \delta\hat{\tau}^2 \rangle$ presented in fig. 7 (circles) decrease linearly with λ as stated in the Introduction, eq. (5). Being a simple mean μ_A (small squares) is found to be strictly λ -independent. As expected, $\mu_{\tau\tau} \rightarrow \mu_A$ for $\lambda \rightarrow 0$. Using eq. (5) the generalized stress-fluctuation

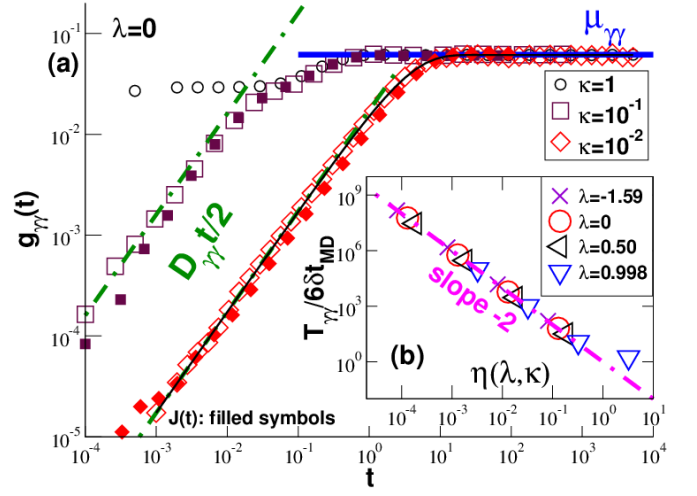


FIG. 8: Diffusion of instantaneous strain $\hat{\gamma}(t)$: (a) MSD $g_{\gamma\gamma}(t)$ for $\lambda = 0$ (open symbols) compared to the explicitly computed creep compliance $J(t) = \langle \delta\hat{\gamma}(t) \rangle / \delta\tau_{\text{ext}}$ for a step stress $\delta\tau_{\text{ext}} = 0.01$ (filled symbols). The dash-dotted lines indicate the regime used to determine the diffusion coefficient $D_{\gamma\gamma}$, the bold horizontal line the expected asymptotic limit $\mu_{\gamma\gamma}$ and the thin solid line the Kelvin-Voigt model, eq. (40), for $\kappa = 10^{-2}$. (b) Double-logarithmic representation of the rescaled crossover time $T_{\gamma\gamma}/6\delta t_{\text{MD}}$ vs. η . The dash-dotted line indicates the expected power law, eq. (60).

formula for G_{eq} reads

$$G_{\tau\tau} \equiv \frac{\mu_A - \mu_{\tau\tau}}{1 - (\mu_A - \mu_{\tau\tau})/G_{\text{ext}}} \text{ for } \lambda \neq 0. \quad (64)$$

For $\lambda \rightarrow 1$, i.e. $G_{\text{ext}} \rightarrow \infty$, this reduces to eq. (16). Equation (64) thus generalizes the stress-fluctuation formula for the NV γ T-ensemble [4, 8–10, 21–23, 33] to general λ . As seen from fig. 7 (diamonds), it is thus possible to determine G_{eq} from μ_A and $\mu_{\tau\tau}$ for all $\lambda \neq 0$.

B. Dynamics: Strain-strain correlations

Strain-strain MSD. The strain histograms $p(x)$ for different λ and their second moments shown, respectively, in fig. 4 and fig. 5 have been rapidly sampled by averaging over short time series from trajectories of length $t_{\text{traj}} = 10^4$. This is demonstrated in panel (c) of fig. 5 presenting the MSD $g_{\gamma\gamma}(t)$ of the instantaneous strain $\hat{\gamma}(t)$ for $\kappa = 10^{-1}$. The statistics is improved by performing a gliding average over the 10^8 data tuples sampled [1]. It is seen that $g_{\gamma\gamma}(t)$ converges rapidly after a time $T_{\gamma\gamma}$ of order unity to its asymptotic limit $\mu_{\gamma\gamma}(\lambda)$ indicated by horizontal lines. Free diffusion is observed for short times, i.e. $g_{\gamma\gamma}(t) \approx D_{\gamma\gamma}t/2$ for $t \ll T_{\gamma\gamma}$ (dash-dotted line), and this essentially irrespective of the ensemble in agreement with eq. (59). Note that free strain diffusion is observed for all λ and sufficiently small κ if the parameter $\eta(\lambda, \kappa) \ll 1$. As shown in the main panel of fig. 8 for different κ and $\lambda = 0$ (open symbols), this behavior

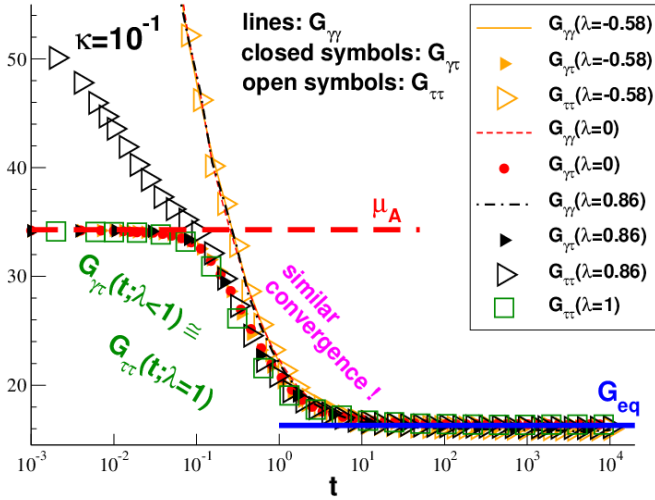


FIG. 9: Determination of equilibrium shear modulus G_{eq} as a function of the sampling time t for $G_{\gamma\gamma}(t)$ (thin lines), $G_{\gamma\tau}(t)$ (filled symbols) and $G_{\tau\tau}(t)$ (large open symbols) for $\kappa = 10^{-1}$. All fluctuation formulae are equivalent for $t > 1$ and converge similarly to G_{eq} for large times. Note that $G_{\gamma\tau}(t)$ for all $\lambda < 1$ is everywhere identical to $G_{\tau\tau}(t)$ for $\lambda = 1$.

may be used to determine first the short-time diffusion coefficient $D_{\gamma\gamma}$ for systems with sufficiently small η and then using eq. (28) the crossover time $T_{\gamma\gamma}$ of the strain fluctuations. The rescaled times $T_{\gamma\gamma}/6\delta t_{\text{MD}}$ are represented in panel (b) of fig. 8 as a function of the scaling variable η for several λ . The dash-dotted line indicates the power-law slope, eq. (60). A perfect data collapse on this line is observed for all $\eta \ll 1$. A successful data collapse can be also obtained for $g_{\gamma\gamma}(t)$ over a broad range of λ and κ by plotting $g_{\gamma\gamma}(t)/\mu_{\gamma\gamma}$ as a function of the reduced time $x = t/T_{\gamma\gamma}$ (not shown). As seen by the thin solid line in the main panel of fig. 8, one verifies that the scaling function $f(x) = g_{\gamma\gamma}(t)/\mu_{\gamma\gamma}$ is given by $f(x) = 1 - \exp(-x)$. This is, of course, consistent with an exponentially decaying strain-strain relaxation function $C_{\gamma\gamma}(t) = \mu_{\gamma\gamma} \exp(-x)$ as we have also checked directly.

Creep compliance $J(t)$. As discussed in sect. IIE, a MSD $g_{\gamma\gamma}(t)$ computed in the NV τ T-ensemble corresponds to a creep compliance $J(t) = \langle \delta\hat{\gamma}(t) \rangle / \delta\tau_{\text{ext}}$ measured by imposing at $t = 0$ a step stress increment $|\delta\tau_{\text{ext}}| \ll 1$ to the external shear stress τ_{ext} applied to the system. Using $\delta\tau_{\text{ext}} = 0.01$ and averaging over 100 configurations this yields the data shown by the filled symbols in panel (a) of fig. 8 for two values of κ . An excellent data collapse $g_{\gamma\gamma}(t) \approx J(t)$ is observed. While it is natural to use the NV τ T-ensemble for obtaining the creep compliance from the equilibrium fluctuations, it is worthwhile to note that due to the scaling $g_{\gamma\gamma}(t)/\mu_{\gamma\gamma} = f(x)$, $J(t)$ may be also determined from other λ -values.

Time-dependent strain-strain fluctuations. As expected from sect. IIB, the strain-strain fluctuations $\bar{\mu}_{\gamma\gamma}(t)$ computed according to eq. (22) by gliding average from a finite time series increase monotonously with

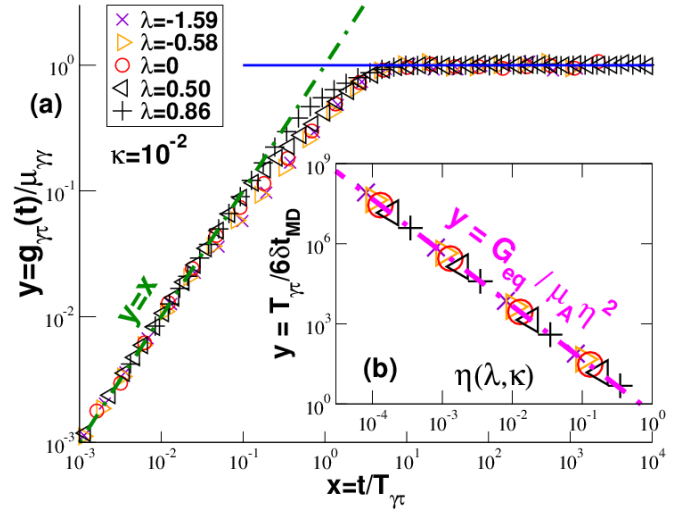


FIG. 10: Scaling of strain-stress MSD $g_{\gamma\tau}(t)$ for different λ : (a) scaling collapse of $y = g_{\gamma\tau}(t)/\mu_{\gamma\tau}$ vs. $x = t/T_{\gamma\tau}$ for $\kappa = 10^{-2}$ with the dash-dotted line indicating the diffusive regime and the bold solid line the long-time limit, (b) crossover time $T_{\gamma\tau}$, eq. (28), rescaled as $T_{\gamma\tau}/6\delta t_{\text{MD}}$ vs. the scaling variable η using the same symbols as in the main panel. The dash-dotted line indicates the prediction eq. (65).

time t from zero (if only one configuration is sampled) to the asymptotic thermodynamic limit $\mu_{\gamma\gamma}$ (not shown). Note that one determines first the strain fluctuations in an interval $[t_0, t_1 = t_0 + t]$ and averages then over all possible t_0 . If the estimate $G_{\gamma\gamma}$, eq. (62), of the modulus G_{eq} is determined using $\bar{\mu}_{\gamma\gamma}(t)$ instead of $\mu_{\gamma\gamma}$, it becomes a time dependent quantity called $G_{\gamma\gamma}(t)$. As can be seen from fig. 9 for three different λ values, $G_{\gamma\gamma}(t)$ thus becomes a monotonously decreasing function of time (thin lines). Interestingly, $G_{\gamma\gamma}(t)$ appears not to depend on λ . We note finally that using either the large-time asymptotics eq. (27) or, more conveniently, the Debye relation eq. (29), one may determine the relaxation time $\theta_{\gamma\gamma}$ of the strain-strain fluctuations $\bar{\mu}_{\gamma\gamma}(t)$. One verifies that $\theta_{\gamma\gamma} \approx T_{\gamma\gamma}$ holds as expected for an exponentially decaying correlation function (sect. IIC).

C. Dynamics: Strain-stress correlations

Strain-stress MSD. The scaling of the strain-stress MSD $g_{\gamma\tau}(t)$ is investigated in fig. 10. The relaxation time $T_{\gamma\tau}$ presented in panel (b) has been determined, as before for $T_{\gamma\gamma}$, by matching the short-time diffusive regime with the long-time limit $g_{\gamma\tau}(t) \rightarrow \mu_{\gamma\tau}$. As indicated by the dash-dotted line, the data are well described by

$$T_{\gamma\tau} = \frac{G_{\text{eq}}}{\mu_A} T_{\gamma\gamma} \sim 1/\kappa^2 \text{ for } \eta \ll 1. \quad (65)$$

That this scaling must hold can be seen by replacing in the definition of $g_{\gamma\tau}(t)$ the stress fluctuation $\delta\hat{\tau}(t)$ by $\mu_A \delta\hat{\gamma}(t)$ which implies $D_{\gamma\tau} = \mu_A D_{\gamma\gamma}$ for the diffusion

coefficients and in turn eq. (65) using again eq. (28). We stress that in agreement with the inset of fig. 6 the system has not enough time to relax the affine strain imposed by the shear-barostat for the short times $t \ll \tau_A \approx 0.1$ considered here. It is thus μ_A and not G_{eq} which has to be used as the linear slope coefficient. The main panel (a) presents the collapse of $y = g_{\gamma\tau}(t)/\mu_{\gamma\tau}$ as a function of $x = t/T_{\gamma\tau}$ for $\kappa = 10^{-2}$. Minor deviations are visible for $x \approx 1$. The quality of the collapse improves by decreasing $\eta(\lambda, \kappa)$, whereas the crossover becomes more sudden (even a hump may occur) if η is too large (not shown).

Time-dependent correlation coefficient $G_{\gamma\tau}(t)$. Since the strain-shear correlations are dominated for $t \ll \tau_A$ by the *affine* shearing, one expects $G_{\gamma\tau}(t)$ computed using the ratio of $\bar{\mu}_{\gamma\tau}(t)$ and $\bar{\mu}_{\gamma\dot{\gamma}}(t)$ to be similar to μ_A for $t \rightarrow 0$. As one sees from $G_{\gamma\tau}(t)$ presented in fig. 9 (filled symbols), this is indeed the case. Interestingly, $G_{\gamma\tau}(t)$ is seen to be independent of λ for *all* times t , i.e. the λ -dependences of $\bar{\mu}_{\gamma\tau}(t)$ and $\bar{\mu}_{\gamma\dot{\gamma}}(t)$ do cancel for all times just as they cancel for the ratio of the equilibrium moments $\mu_{\gamma\tau}/\mu_{\gamma\dot{\gamma}}$.

D. Dynamics: Stress-stress correlations

Introduction. We turn finally to the more intricate characterization of the stress-stress correlations as a function of our two operational parameters λ and κ . We focus again on the regime with $\eta(\lambda, \kappa) \ll 1$. As above we begin by discussing the MSD $g_{\tau\tau}(t)$. Since according to eq. (20)

$$g_{\tau\tau}(t) = C_{\tau\tau}(0) - C_{\tau\tau}(t) \text{ with } C_{\tau\tau}(0) = \mu_{\tau\tau}, \quad (66)$$

the MSD $g_{\tau\tau}(t)$ and the correlation function $C_{\tau\tau}(t)$ contain in principal the same information. From the presentational point of view $g_{\tau\tau}(t)$ has the advantage that the short-time power-law behavior of the correlations can be made manifest using a double-logarithmic plot as shown in fig. 11. We describe then the large time behavior of the correlation function $C_{\tau\tau}(t)$ and demonstrate that τ_* is given by $T_{\gamma\dot{\gamma}}$. Finally, we turn to the time-dependent stress fluctuation $\bar{\mu}_{\tau\tau}(t)$ which is used to determine the stress-stress relaxation time $\theta_{\tau\tau}$.

Stress-stress MSD. Let us concentrate first on the data for $\lambda = -1.59$ presented by open symbols in fig. 11. If κ is large, all internal dynamics is destroyed and we find immediately $g_{\tau\tau}(t) \approx \mu_{\tau\tau}$ as seen for $\kappa = 1$ (small circles). For smaller, but not too small κ one observes a free-diffusion regime with $g_{\tau\tau}(t) = D_{\tau\tau}t/2$ as shown by the bold dash-dotted lines on the left. As above for $g_{\gamma\tau}(t)$ in sect. IV C, $\delta\hat{\tau}(t)$ in the definition of $g_{\tau\tau}(t)$ can be replaced by $\mu_A\delta\hat{\gamma}(t)$. This argument yields the diffusion coefficient $D_{\tau\tau} = \mu_A^2 D_{\gamma\dot{\gamma}}$ successfully used in the plot for $\kappa = 10^{-1}$ and $\kappa = 10^{-2}$. If κ is further reduced, $g_{\tau\tau}(t)$ becomes κ -independent for short times. As seen for $\kappa = 10^{-3}$ and 10^{-4} the dynamics becomes “deterministic” in the sense that

$$g_{\tau\tau}(t) = \frac{\mu_{\tau\tau}}{2} (t/\tilde{\theta})^2 \sim \kappa^0 \lambda^0 \text{ for } t \ll \tau_A \quad (67)$$

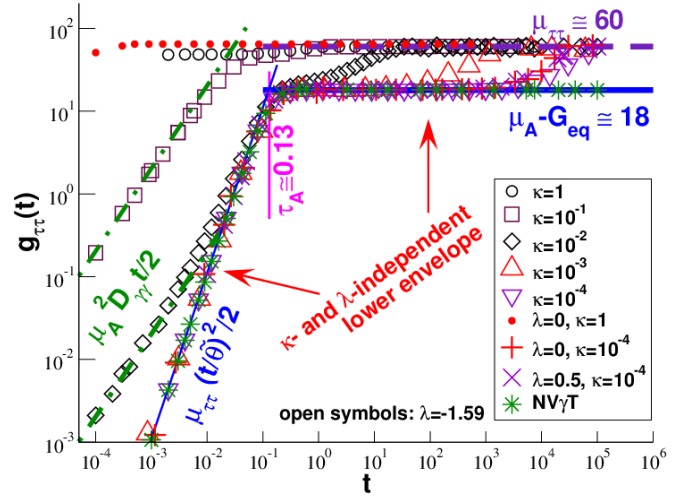


FIG. 11: Stress-stress MSD $g_{\tau\tau}(t)$ focusing on $\lambda = -1.59$ comparing different κ (open symbols). Additionally, we present $\lambda = 0$ for $\kappa = 1$ (small filled circles) and $\kappa = 10^{-4}$, $\lambda = 0.5$ for $\kappa = 10^{-4}$ and the NV γ T-ensemble (stars). The dot-dashed lines indicate the free diffusive behavior for intermediate η , the thin solid line the analytic short-time limit for small η , the horizontal dashed line the thermodynamic limit $\mu_{\tau\tau}$ for $\lambda = -1.59$ and the bold solid line the expected intermediate plateau, eq. (38). Note that for sufficiently small κ all data approach the κ - and λ -independent lower envelope indicated by the solid lines in agreement with the fundamental scaling postulate eq. (31).

with $\tilde{\theta} \approx 0.16$ as shown by the thin solid line. Albeit $\mu_{\tau\tau}$ depends on λ , the ratio $\mu_{\tau\tau}/\tilde{\theta}^2$ does not, in agreement with the fundamental postulate eq. (31). This implies that $\tilde{\theta}$ depends somewhat on λ . The t^2 -scaling in eq. (67) is expected [10] since the associated correlation function $C_{\tau\tau}(t)$ must be a continuous and symmetric function at $t = 0$ which, moreover, should be an *analytic* function if barostat and thermostat effects can be ignored [35]. This implies that $g_{\tau\tau}(t)$ must be an even expansion in terms of t^2 which to leading order leads to eq. (67). Since there are several dynamical regimes it is not meaningful to determine a crossover time $T_{\tau\tau}$ using eq. (28) as before for $T_{\gamma\dot{\gamma}}$ and $T_{\gamma\tau}$ over the full range of λ and κ . We shall see at the end of this section how a longest relaxation time $\theta_{\tau\tau}$ for the stress-stress correlations might be obtained. For times $t \gg \tau_A$ an intermediate plateau appears (bold solid line) as predicted by eq. (37). As can be seen for four different λ values this intermediate plateau does *not* depend on the ensemble provided that κ is sufficiently weak. (As one expects from fig. 3 deviations from this asymptotic limit arise again for large κ if $\eta(\lambda, \kappa) \gg 0.1$.) We emphasize that the two solid lines indicated in fig. 11 give the lower envelope for all parameters λ and κ we have simulated. The MSD $g_{\tau\tau}(t)$ behaves thus as an ensemble-independent simple average as we have argued in sect. IID. One may operationally define the crossover

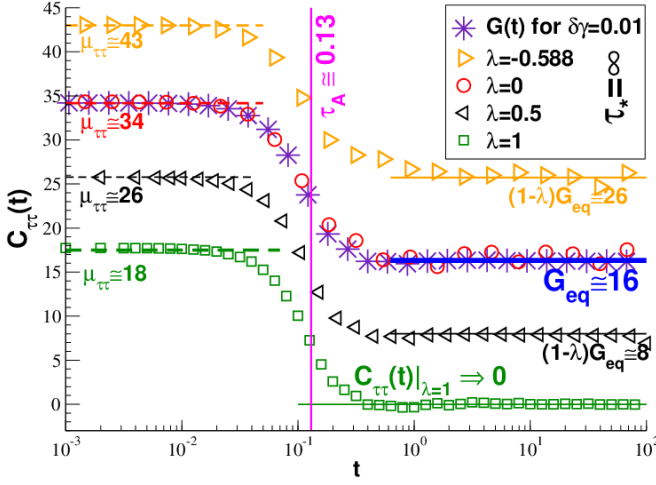


FIG. 12: Relaxation modulus $G(t)$ obtained from the stress response to an applied strain $\delta\gamma = 0.01$ (stars) compared to the equilibrium correlation function $C_{\tau\tau}(t)|_{\lambda}$ for several λ obtained by averaging over 1000 quenched-strain configurations.

time τ_A by matching eq. (67) and eq. (38). This yields

$$\tau_A = \tilde{\theta} \sqrt{2 \frac{1 - G_{\text{eq}}/\mu_A}{1 - \lambda G_{\text{eq}}/\mu_A}} \approx 0.13 \quad (68)$$

as indicated by the vertical line. Note that $\tau_A = \tilde{\theta}\sqrt{2}$ for $\lambda = 1$. We stress that while $\tilde{\theta}$ is a function of λ , τ_A is an ensemble-independent constant for the given elastic network. (Moreover, it can be shown that it barely depends on the friction constant ζ of the Langevin thermostat [10].) Using eq. (68) one may reformulate eq. (67) in a manifest λ -independent form: $g_{\tau\tau}(t) = (\mu_A - G_{\text{eq}}) (t/\tau_A)^2$. The MSD ultimately approaches $\mu_{\tau\tau}(\lambda)$ for even larger times $t \gg \tau_*$ as indicated by the dashed horizontal line for $\lambda = -1.59$. Remembering that $\mu_{\tau\tau} = \mu_A - G_{\text{eq}}$ for $\lambda = 1$ it is clear that the NV γ T-data stays constant for all times.

Relaxation modulus. The large- t scaling is further addressed in fig. 12 and fig. 13 presenting the stress-stress correlation function $C_{\tau\tau}(t)$. The most central result of this work stated by eq. (6) is demonstrated in fig. 12. We compare the directly measured relaxation modulus $G(t)$ with the equilibrium correlation function $C_{\tau\tau}(t)$ assuming an asymptotically slow barostat ($\tau_* = \infty$). Averaging over 1000 independent configurations from an NV γ T-ensemble with $\gamma = 0$ for $t < 0$, the relaxation modulus $G(t) = \langle \hat{\tau}(t) \rangle / \delta\gamma$ measures the stress response after a (canonical and affine) shear strain $\delta\gamma = 0.01$ was been applied at $t = 0$ (stars). The correlation functions $C_{\tau\tau}(t)$ for $\lambda < 1$ have been obtained by averaging over 1000 equilibrated configurations from a λ -ensemble as indicated. Switching off the shear-barostat the strain $\hat{\gamma}$ of each configuration is quenched. Note that $C_{\tau\tau}(0) = \mu_{\tau\tau}$ holds due to the ensemble averaging. As expected from eq. (37), $C_{\tau\tau}(t)$ decreases monotonously from $\mu_{\tau\tau}$ down

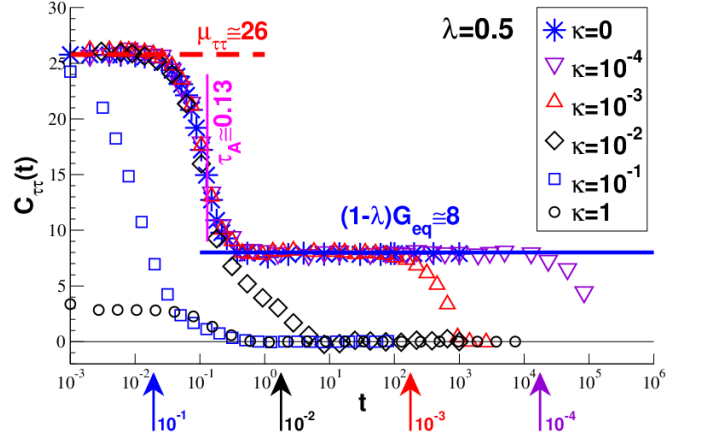


FIG. 13: Effect of the barostat parameter κ for $C_{\tau\tau}(t)$ with $\lambda = 0.5$. The large stars correspond to the quenched γ -ensemble ($\tau_* = \infty$) and all other symbols to a switched-on barostat of finite κ . The vertical arrows indicate $T_{\gamma\gamma}$ for $\kappa = 10^{-1}, 10^{-2}, 10^{-3}$ and 10^{-4} confirming that roughly $T_{\gamma\gamma} \approx \tau_*$. A much longer run is warranted for $\kappa = 10^{-4}$.

to $(1 - \lambda)G_{\text{eq}}$ for $t \gg \tau_A$. This corresponds to the λ -independent intermediate plateau $g_{\tau\tau}(t) = \mu_A - G_{\text{eq}}$ in fig. 11. It is seen that $G(t) = C_{\tau\tau}(t)$ for $\lambda = 0$ (large circles) and that for all λ one may obtain $G(t)$ by vertically shifting the correlation functions $C_{\tau\tau}(t)|_{\lambda} \rightarrow C_{\tau\tau}(t)|_{\lambda} + \lambda G_{\text{eq}} = G(t)$ using the already determined shear modulus G_{eq} . Note also that $C_{\tau\tau}(t)|_{\lambda=1} \rightarrow 0$ for large times while all other $C_{\tau\tau}(t)$ remain finite. As already emphasized at the end of sect. II E, it is thus impossible to obtain the modulus G_{eq} solely from $C_{\tau\tau}(t)|_{\lambda=1}$. Please note that the observed short-time value $\mu_{\tau\tau} \approx 18$ (bold dashed line) for $\lambda = 1$ is quite different from the equilibrium modulus $G_{\text{eq}} \approx 16$ (bold solid line).

Finite- κ effects. Focusing on one ensemble with $\lambda = 0.5$ we investigate in fig. 13 the effect of a switched-on shear barostat. The stars refer to data already seen in fig. 12 using the quenched-strain ensemble ($\kappa = 0$, $\tau_* = \infty$). As one expects, the decay of $C_{\tau\tau}(t)$ becomes systematically slower with decreasing κ . For large $\kappa > 10^{-2}$ we have computed $C_{\tau\tau}(t)$ by gliding averaging over a single trajectory of $t_{\text{traj}} = 10^4$. For smaller κ it becomes increasingly harder to have a sufficiently long trajectory of $\{\hat{\tau}_k\}$ probing the phase space, i.e. for which $C_{\tau\tau}(0) = \mu_{\tau\tau}$, and to store at the same time the shear stresses with a sufficiently fine time resolution. The data for $\kappa \leq 10^{-2}$ have thus been obtained by using an ensemble of 100 configurations of different $\hat{\gamma}$ and averaging over the trajectories obtained for each configuration using a finite κ . As expected from eq. (37), for sufficiently small κ all correlation functions have an intermediate plateau for $\tau_A \ll t \ll \tau_*$ (bold solid line). That the barostat is not completely switched off can be seen from the final decay. The vertical arrows indicate the crossover times $T_{\gamma\gamma}$ for the four smallest κ . As one expects, this time scale appears to coincide roughly (up to a constant prefactor) with the upper limit τ_* of the respective plateau. In other

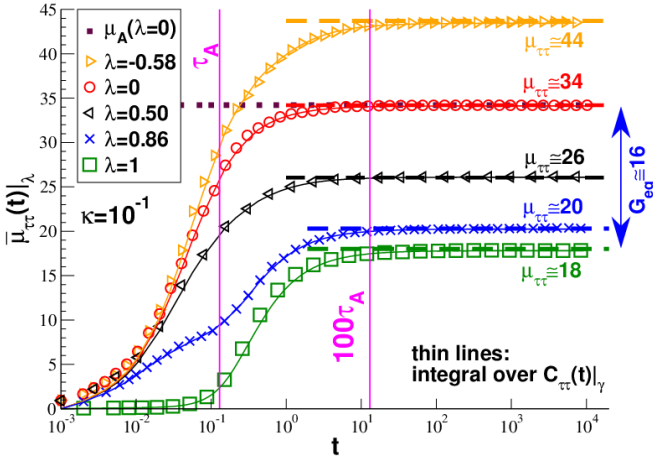


FIG. 14: Shear-stress fluctuation $\bar{\mu}_{\tau\tau}(t)|_{\lambda}$ as a function of the sampling time. Also indicated is the affine shear-elasticity μ_A obtained for the NV τ T-ensemble (small filled squares) which is seen to immediately converge to the long-time limit. The thin lines correspond to the integrated shear-stress auto-correlation function $C_{\tau\tau}(t)|_{\lambda}$ according to eq. (25).

words, the plateau disappears when the ergodicity breaking associated with the averaging over a quenched-strain ensemble is lifted by the shear-barostat.

Time-dependent stress-fluctuation formula. Let us return to fig. 9. According to the generalized stress-fluctuation formula $G_{\tau\tau}$, eq. (64), the shear modulus G_{eq} may be obtained from the affine shear-elasticity μ_A and the equilibrium stress-stress fluctuation $\mu_{\tau\tau}$ for $\lambda \leq 1$ and $\lambda \neq 0$ (fig. 7). If instead of $\mu_{\tau\tau}$ a time-averaged fluctuation $\bar{\mu}_{\tau\tau}(t)$ is used, this leads again to a time-dependent monotonously decreasing estimate $G_{\tau\tau}(t)$ as seen from the open symbols in fig. 9. No shear-barostat is of course applied for the NV γ T-ensemble indicated by the large squares. We emphasize the remarkable finding that within numerical accuracy

$$G_{\tau\tau}(t)|_{\lambda=1} \approx G_{\gamma\tau}(t)|_{\lambda<1} \quad (69)$$

for all times and a broad range of κ for $G_{\gamma\tau}(t)$. As seen for $\lambda = -0.58$, for small λ and not too short times $G_{\tau\tau}(t)$ and $G_{\gamma\gamma}(t)$ are generally similar. Since $\bar{\mu}_{\tau\tau}(t)$ must vanish for small times, this implies that $G_{\tau\tau}(t)$ must become finite

$$G_{\tau\tau}(t) \rightarrow \frac{\mu_A}{1 - \mu_A/G_{ext}} \quad \text{for } t \rightarrow 0 \quad (70)$$

and, hence, $G_{\tau\tau}(t) \rightarrow \mu_A$ for $G_{ext} \gg \mu_A$. This limit is indicated by the bold dashed line for $\lambda = 1$.

Time-dependence of stress-stress fluctuations. The time-dependence of $\bar{\mu}_{\tau\tau}(t)$ for several λ is explicitly represented in fig. 14 assuming $\kappa = 10^{-1}$ for $\lambda < 1$. While the simple mean μ_A converges immediately with time, $\bar{\mu}_{\tau\tau}(t)$ increases monotonously from zero to the large-time limit $\mu_{\tau\tau}$ (horizontal lines). As already pointed out in sect. IIB, assuming time-translational invariance the time-dependence of $\bar{\mu}_{\tau\tau}(t)$ is a consequence of the time-dependence of the $C_{\tau\tau}(t)$. To emphasize this point we

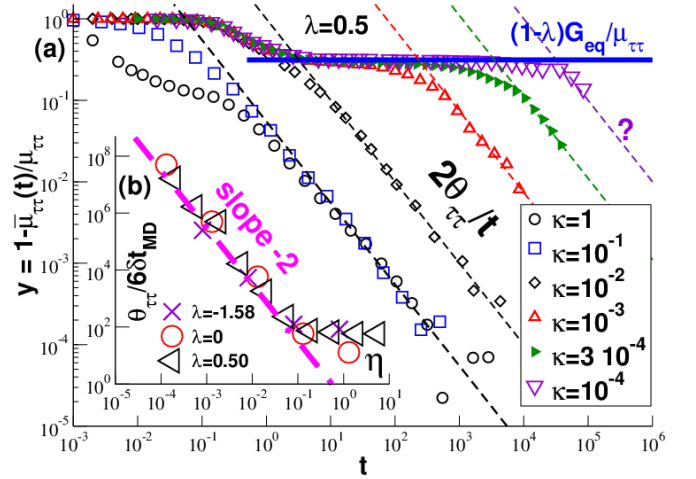


FIG. 15: Stress-stress relaxation time $\theta_{\tau\tau}$: (a) Determination of $\theta_{\tau\tau}$ from the decay of $y = 1 - \bar{\mu}_{\tau\tau}(t)/\mu_{\tau\tau}$ according to eq. (27) for $\lambda = 0.5$ for different κ . The thin dashed lines indicate eq. (27), the bold horizontal line the expected intermediate plateau $(1 - \lambda)G_{eq}/\mu_{\tau\tau}$ for $10\tau_A \ll t \ll \tau_*$. (b) Relaxation time $\theta_{\tau\tau}$ for three not too large λ plotted as $\theta_{\tau\tau}/6\delta t_{MD}$ vs. $\eta(\lambda, \kappa)$. The dash-dotted line indicates the power law expected for $\eta \ll 1$ according to eq. (71).

have integrated $C_{\tau\tau}(t)$ as suggested by eq. (25). As seen by the thin lines indicated in fig. 14, this leads to consistent results. If one has thus characterized $C_{\tau\tau}(t)$, this implies $\bar{\mu}_{\tau\tau}(t)$ and then in turn $G_{\tau\tau}(t)$. Note that for all λ the asymptotic limit is reached at about $100\tau_A$ which is of the same order as $T_{\gamma\gamma} \approx 3.5$ for $\lambda = 0$ and $\kappa = 10^{-1}$.

Relaxation time $\theta_{\tau\tau}$. The convergence of $\bar{\mu}_{\tau\tau}(t)$ is systematically analyzed in fig. 15. The main panel presents the dimensionless deviation $y = 1 - \bar{\mu}_{\tau\tau}(t)/\mu_{\tau\tau}$ for several κ and $\lambda = 0.5$. As emphasized by the thin dashed lines, a correlation time $\theta_{\tau\tau}$ may be measured from the large-time $1/t$ -decay following eq. (27). (Unfortunately, the sampling time is yet insufficient for our smallest κ .) With decreasing κ the decay becomes systematically slower and a horizontal plateau with $y = (1 - \lambda)G_{eq}/\mu_{\tau\tau}$ (bold solid line) appears in an intermediate time window. This plateau is expected from eq. (30) and eq. (37). Following the discussion in sect. IIB, this implies that for sufficiently small κ and not too large λ the relaxation time $\theta_{\tau\tau}$ must scale (up to a prefactor of order unity) as

$$\theta_{\tau\tau} \approx \frac{(1 - \lambda)G_{eq}}{\mu_{\tau\tau}} \tau_* \sim (1 - \lambda)^2/\kappa^2 \quad \text{for } \eta \ll 1 \quad (71)$$

to leading order where we have used eq. (60) for $\tau_* \approx T_{\gamma\gamma} \sim 1/\kappa^2$. That the κ -scaling holds can be seen in panel (b) of fig. 15. (For $\lambda = 0.5$ we have computed $\theta_{\tau\tau}$ also for the additional values $\kappa = 3, 0.3, 0.03, 0.003$ and 0.0003 .) The same representation as in the insets of figs. 8 and 10 has been chosen for comparison. It should be stressed, however, that for $\theta_{\tau\tau}$ this is for two reasons not a rigorous scaling plot over the full range of operational parameters considered. Firstly, due to the

$(1-\lambda)G_{\text{eq}}/\mu_{\tau\tau}$ -factor in eq. (71) there is an additional λ -dependence even for $\eta \ll 1$ and not too large λ . (This can be accounted for using a different representation.) More importantly, for $\lambda \approx 1$ barostat effects naturally become irrelevant and the intrinsic relaxation time τ_A essentially sets $\theta_{\tau\tau}$ and not $\tau_* \approx T_{\gamma\gamma}$. We thus observe $\theta_{\tau\tau} \approx \tau_A \lambda^0 \kappa^0$ for all $\lambda > 0.8$ as seen in table I for $\kappa = 10^{-2}$. Basically, since we have *two* time scales τ_A and $T_{\gamma\gamma}$, it is not possible to put all $\theta_{\tau\tau}(\lambda, \kappa)$ on *one* master curve.

V. CONCLUSION

Static properties. Focusing on two-dimensional elastic networks (sect. III) we have characterized theoretically (sect. II) and numerically (sect. IV) the static and dynamical fluctuations of shear-strain and shear-stress in generalized Gaussian ensembles as a function of the dimensionless parameter $\lambda = G_{\text{ext}}/(G_{\text{eq}} + G_{\text{ext}})$, fig. 1. Monitoring various properties we interpolate between the NV γ T-ensemble ($\lambda = 1$) and the NV τ T-ensemble ($\lambda = 0$) and consider even negative λ . The static strain-strain fluctuations $\mu_{\gamma\gamma}$ (fig. 5), the strain-stress fluctuations $\mu_{\gamma\tau}$ and the stress-stress fluctuations $\mu_{\tau\tau}$ (fig. 7) have been shown to decrease linearly with increasing λ [20]. As a consequence, the static shear modulus G_{eq} may be obtained (fig. 7) from either the strain-strain fluctuation formula $G_{\gamma\gamma}$, eq. (62), or from the strain-stress formula $G_{\gamma\tau}$, eq. (63), for $\lambda < 1$ or the stress-stress fluctuation formula $G_{\tau\tau}$, eq. (64), for $\lambda \neq 0$. The latter formula is a generalization of the well-known stress-fluctuation formula eq. (16) for $\lambda = 1$. When sampled from a *finite* time series $(\hat{\gamma}_k, \hat{\tau}_k)$, $G_{\gamma\gamma}(t)$, $G_{\gamma\tau}(t)$ and $G_{\tau\tau}(t)$ behave similarly with time t for all λ (fig. 9). Interestingly, $G_{\tau\tau}(t)|_{\lambda=1}$ and $G_{\gamma\tau}(t)|_{\lambda<1}$ are identical for *all* times.

Dynamic properties. The influence of the parameter κ of the MC shear-barostat (sect. III E) has been investigated for various dynamical properties, especially for the stress-stress correlation function $C_{\tau\tau}(t)$ (fig. 13). The upper time limit $\tau_*(\lambda)$, below which barostat effects can be ignored, is set by the strain-strain crossover time $T_{\gamma\gamma}(\lambda)$ (fig. 8). While a rapid barostat may be of advantage for static properties, a sufficiently slow barostat with a large τ_* corresponds to the fundamentally important linear-response limit where the barostat is only relevant for the distribution of the start points of the trajectories

(and, hence, $C_{\text{ab}}(0) = \mu_{\text{ab}}$) but *not* for their dynamical pathways for $t \ll \tau_*$. We have argued that this implies the fundamental scaling $g_{\text{ab}}(t) \sim \lambda^0 \kappa^0$ for $t \ll \tau_*(\lambda)$ as demonstrated explicitly for $g_{\tau\tau}(t)$ in fig. 11. Assuming such a slow barostat one may obtain G_{eq} using eq. (6) from $C_{\tau\tau}(t)|_{\lambda} \approx (1-\lambda)G_{\text{eq}}$ for $\lambda < 1$ (fig. 12). As emphasized elsewhere [9, 10], it is impossible, however, to obtain the modulus G_{eq} *alone* from the autocorrelation function $C_{\tau\tau}(t)|_{\lambda=1}$. The experimentally important shear-stress relaxation modulus $G(t)$ may be most readily determined at $\lambda = 1$ calculating first $G_{\text{eq}} = \mu_A - \mu_{\tau\tau}|_{\lambda=1}$ and then $G(t) = C_{\tau\tau}(t)|_{\lambda=1} + G_{\text{eq}}$ [36]. We have commented briefly on the creep compliance $J(t)$. Being well-described by the Kelvin-Voigt model, eq. (40), $J(t)$ is best obtained from the strain-strain MSD $g_{\gamma\gamma}(t)$ at $\lambda = 0$ (fig. 8).

More general thermodynamic variables. Most of the theoretical relations and numerical techniques discussed above, especially the key formulae eq. (5) and eq. (6), generalize readily for any pair of *continuous* extensive and intensive variables X and I with $M_{\text{eq}} = \partial I / \partial X$ being the equilibrium modulus. With M_{ext} being the spring constant of the external potential controlling the fluctuations of the extensive variable and $\lambda = M_{\text{ext}} / (M_{\text{eq}} + M_{\text{ext}})$ one obtains, e.g., the relaxation modulus

$$M(t) = C(t)|_{\lambda=0} = C(t)|_{\lambda} + \lambda M_{\text{eq}} \quad \text{for } t \ll \tau_*(\lambda) \quad (72)$$

with $C(t) \equiv \beta V \langle \delta \hat{I}(t) \delta \hat{I}(0) \rangle$ being the relevant autocorrelation function. The associated MSD $g(t) \equiv (\beta V / 2) \langle (\hat{I}(t) - \hat{I}(0))^2 \rangle$ is expected to be strictly λ -independent in the same time window. These properties must be computed again either using a slow “barostat” with a large, albeit finite $\tau_* \ll t_{\text{traj}}$ or, equivalently, by averaging over an equilibrium ensemble of configurations with frozen \hat{X} . For times $t \gg \tau_*$ a switched-on “barostat” ultimately restores the ergodicity and $C(t)$ must vanish while $g(t)$ approaches its finite thermodynamic value $\beta V \langle \delta \hat{I}^2 \rangle$.

Acknowledgments

H. Xu thanks the IRTG Soft Matter for financial support. We are indebted to O. Benzerara (Strasbourg) and J. Helfferich (Freiburg) for helpful discussions.

-
- [1] M. Allen and D. Tildesley, *Computer Simulation of Liquids* (Oxford University Press, Oxford, 1994).
 - [2] J. L. Lebowitz, J. K. Percus, and L. Verlet, *Phys. Rev.* **153**, 250 (1967).
 - [3] H. B. Callen, *Thermodynamics and an Introduction to Thermostatistics* (Wiley, New York, 1985).
 - [4] D. Frenkel and B. Smit, *Understanding Molecular Simulation – From Algorithms to Applications* (Academic Press, San Diego, 2002), 2nd edition.
 - [5] D. P. Landau and K. Binder, *A Guide to Monte Carlo Simulations in Statistical Physics* (Cambridge University Press, Cambridge, 2000).
 - [6] J. Thijssen, *Computational Physics* (Cambridge University Press, Cambridge, 1999).
 - [7] M. Born and K. Huang, *Dynamical Theory of Crystal Lattices* (Clarendon Press, Oxford, 1954).
 - [8] J. P. Wittmer, H. Xu, P. Polińska, F. Weysser, and J. Baschnagel, *J. Chem. Phys.* **138**, 12A533 (2013).

- [9] J. P. Wittmer, H. Xu, and J. Baschnagel, *Phys. Rev. E* **91**, 022107 (2015).
- [10] J. P. Wittmer, H. Xu, O. Benzerara, and J. Baschnagel, *Mol. Phys.* **113**, 10.1080/00268976.2015.1023225 (2015).
- [11] J. Hansen and I. McDonald, *Theory of simple liquids* (Academic Press, New York, 2006), 3rd edition.
- [12] J. Hetherington, *J. Low Temp. Phys.* **66**, 145 (1987).
- [13] M. Costeniuc, R. Ellis, H. Touchette, and B. Turkington, *Phys. Rev. E* **73**, 026105 (2006).
- [14] K. van Workum and J. de Pablo, *Phys. Rev. E* **67**, 011505 (2003).
- [15] The focus of Hetherington's Gaussian ensemble [12], as of related generalizations [13], is on the transformation between the *microcanonical ensemble*, characterized by the (possibly non-concave) entropy as a function of the energy, and the (generalized) *canonical ensemble*, characterized by the free energy as function of the inverse temperature β , i.e. different pairs of conjugated variables are considered compared to the present work.
- [16] T. Witten and P. A. Pincus, *Structured Fluids: Polymers, Colloids, Surfactants* (Oxford University Press, Oxford, 2004).
- [17] M. Rubinstein and R. Colby, *Polymer Physics* (Oxford University Press, Oxford, 2003).
- [18] J. P. Wittmer, H. Xu, P. Políńska, C. Gillig, J. Helfferich, F. Weysser, and J. Baschnagel, *Eur. Phys. J. E* **36**, 131 (2013).
- [19] The observable becomes T -independent at low temperatures due to the prefactor $\beta = 1/T$ and system size independent due to the prefactor V .
- [20] Using the slightly modified definitions $\tilde{\mu}_{\gamma\gamma} = \mu_{\gamma\gamma}G_{\text{eq}}$, $\tilde{\mu}_{\gamma\tau} = \mu_{\gamma\tau}$ and $\tilde{\mu}_{\tau\tau} = \mu_{\tau\tau}/G_{\text{eq}}$, one obtains the general transform $\tilde{\mu}_{\text{ab}}|_{\lambda} = \tilde{\mu}_{\text{ab}}|_{\lambda=0} - \lambda$ for all fluctuations. Similarly, the rescaling $\tilde{C}_{\gamma\gamma}(t) = C_{\gamma\gamma}(t)G_{\text{eq}}$, $\tilde{C}_{\gamma\tau}(t) = C_{\gamma\tau}(t)$ and $\tilde{C}_{\tau\tau}(t) = C_{\tau\tau}(t)/G_{\text{eq}}$ leads to the compact transformation relation $\tilde{C}_{\text{ab}}(t)|_{\lambda} = \tilde{C}_{\text{ab}}(t)|_{\lambda=0} - \lambda$ for the correlation functions. Equation (7) may be generalized as
- $$\frac{d}{d\lambda}\tilde{\mu}_{\text{ab}}|_{\lambda} = \frac{d}{d\lambda}\tilde{C}_{\text{ab}}(t)|_{\lambda} = -1$$
- with appropriate conditions at $\lambda = 0$.
- [21] D. R. Squire, A. C. Holt, and W. G. Hoover, *Physica* **42**, 388 (1969).
- [22] H. Mizuno, S. Mossa, and J.-L. Barrat, *Phys. Rev. E* **87**, 042306 (2013).
- [23] J.-L. Barrat, J.-N. Roux, J.-P. Hansen, and M. L. Klein, *Europhys. Lett.* **7**, 707 (1988).
- [24] J. P. Wittmer, A. Tanguy, J.-L. Barrat, and L. Lewis, *Europhys. Lett.* **57**, 423 (2002).
- [25] A. Tanguy, J. P. Wittmer, F. Leonforte, and J.-L. Barrat, *Phys. Rev. B* **66**, 174205 (2002).
- [26] E. Flenner and G. Szamel, *Phys. Rev. Lett.* **107**, 105505 (2015).
- [27] M. Doi and S. F. Edwards, *The Theory of Polymer Dynamics* (Clarendon Press, Oxford, 1986).
- [28] This assumes that the system is ergodic and does not apply if one samples, e.g., configuration ensembles with quenched shear-strain.
- [29] As seen in fig. 15, in some cases rather long trajectories are needed to determine clearly a relaxation time θ_{ab} from the $1/t$ -decay of $y(t) \equiv 1 - \bar{\mu}_{\text{ab}}(t)/\mu_{\text{ab}}$. As shown in ref. [10] one may instead characterize a relaxation time using $y(t = \theta_f) = f$ with $f \ll 1$ being a fixed fraction, say $f = 1/100$ [10]. If f is sufficiently small, eq. (27) implies $\theta_{\text{ab}} = \theta_f f/2$.
- [30] C. Klix, F. Ebert, F. Weysser, M. Fuchs, G. Maret, and P. Keim, *Phys. Rev. Lett.* **109**, 178301 (2012).
- [31] H. Goldstein, J. Safko, and C. Poole, *Classical Mechanics* (Addison-Wesley, 2001), 3rd edition.
- [32] A prime denotes generally a derivative of a function with respect to its argument.
- [33] J. F. Lutsko, *J. Appl. Phys.* **65**, 2991 (1989).
- [34] For each x one only takes into account $(\hat{\gamma}, \hat{\tau})$ with $\hat{\gamma}$ corresponding to a finite δx -bin around x .
- [35] A good fit for the short time behavior is given by the Gaussian $C_{\tau\tau}(t) = \mu_{\tau\tau} \exp(-(t/\tilde{\theta})^2/2)$ [10]. To leading order this yields eq. (67).
- [36] See ref. [10] for the determination of $G'(\omega)$ and $G''(\omega)$ using an oscillatory shear strain of frequency ω .